

Neutron astronomy

Diego Casadei*

*School of Physics and Astronomy, University of Birmingham
and School of Engineering, FHNW*

(Dated: 9 Jan 2017. Last revision: August 7, 2017)

Neutrons travel along straight lines in free space, but only survive for a distance which depends on their energy. Thus, detecting neutrons in space in principle provides directional and distance information. Apart from secondary neutrons produced by cosmic-ray interactions in the Earth atmosphere, which are the dominant background, direct neutron emission is caused by solar flares, with clear time correlation with X-rays, which can be measured from few tens MeV up to few GeV. There is no detectable astrophysical source up to the PeV scale, when neutrons coming from supernova remnants may reach the Earth before decaying. In addition, ultra high energy neutrons are the most plausible explanation for the measured anisotropy of cosmic-ray showers produced in the atmosphere above 10^{18} eV. From the GeV to the PeV scale, the expected neutron flux is very low and not too different from the antiproton flux, as the same cosmic-ray collisions with the interstellar medium which can produce antiprotons can also produce neutrons and antineutrons. This background flux of cosmic-ray neutrons is very low and has not yet been detected. Measuring the neutron energy spectrum in space is a very effective way of searching for decays of exotic particles. For example, dark matter could consist of Weakly Interacting Massive Particles (WIMPs), which may annihilate into final states with particle and antiparticle pairs. Consequently, a number of indirect WIMP searches are being carried on, focusing on positron and antiproton spectra. However, no experiment is presently foreseen to look for “bumps” in the neutron energy spectrum, which is virtually background free. Here we consider the implications of a measurement of the neutron energy spectrum in astronomy and astrophysics and list the interesting energy regions in the search for WIMPs.

PACS numbers: 95.30.Cq, 95.35.+d, 95.55.-n, 95.55.Vj

Keywords: cosmic rays; neutrons; dark matter

I. INTRODUCTION

Cosmic rays (CR) have been studied since one century with experiments performed on the ground or underground, on high mountains, on stratospheric balloons, and on satellites. They consist mainly of protons ($\sim 90\%$), helium nuclei and electrons, although all elements are also present (see for example [1]). Although the magnetic field intensities are usually very weak in empty space (with the important exceptions of the sites where charged CR get accelerated), the distances traveled between their sources and the Earth are so big that the deviations induced by the magnetic fields completely erase the information about the location of CR sources: no astronomy is possible with charged particles.

On the other hand, neutral particles travel along straight lines, hence provide directional information on the location of their sources. This is the case for photons and neutrinos, for example. Photons can be detected over an enormous energy range, and are the classical carriers for astronomy. They even allow us to achieve 3-dimensional maps, by exploiting the cosmological redshift to date their sources back to the recombination period. In the past few decades a big progress has been achieved on neutrino astrophysics, and huge detectors (necessary because of the very small neutrino

cross-section) are now operating in different locations all around the world.

Among the known particles, neutrons possess very interesting characteristics. They are neutral like photons and neutrinos, hence they travel along straight lines. However, they have a long but finite life time ($\tau_0 = 881.5 \pm 1.5$ s [2]) hence travel for a typical distance of $\gamma c \tau_0$ (more details in section II below), where $\gamma = (1 - v^2/c^2)^{-1/2}$ is the Lorentz factor and $c \tau_0 = 2.64 \times 10^{11}$ m = 1.77 AU = 8.6×10^{-6} pc. Hence there is a typical energy threshold for the neutrons coming from a source at some distance x . Furthermore, most astrophysical sources produce energy spectra which are steeply falling down functions, hence the expected neutron energy distribution may be detectable in a relatively narrow range. This means that neutrons at different energies probe different depths, creating a sort of “astrotomography” of the environment around the observer.

Neutrons from the Sun need to be above about 20 MeV to survive until the Earth and their spectrum steeply falls down at higher energies, such that they are detectable up to several hundred MeV. For larger energies, there is no standard source of neutrons up to the PeV region, where neutrons emitted during supernova explosions may reach the solar system. Thus there is a very wide range, spanning many decades in energy, in which the expected flux of neutrons is very low and so far remained undetected. This is essentially a background-free region for the search for new particles, for example the Weakly In-

* diego.casadei@cern.ch

interacting Massive Particles (WIMPs), which are among the favored dark matter candidates.

At present, several space experiments (like AMS-02 and DAMPE, for example) are looking for the signatures of WIMP decays in the proton-antiproton and electron-positron final states. As a neutron-antineutron final state is essentially equivalent to a proton-antiproton decay (both come from hadronization of a quark-antiquark pair), it comes out that WIMP searches may also be carried on by focusing on the energy spectrum of cosmic neutrons. The advantage is that the only source of instrumental background is connected to the cosmic gamma rays and to the secondary neutrons produced in the spacecraft and in the Earth atmosphere: an anticoincidence shield is sufficient to get rid of all charged particles (in particular of CR protons). By exploiting pulse shape discrimination techniques, the gamma-ray background can be easily suppressed. In addition, a directional neutron detector can easily get rid of the atmospheric background (alternatively one could perform a differential measurement between upward and downward going neutrons), leaving only the diffuse cosmic neutrons as background sources. The flux of cosmic neutrons is so low that one is left almost with a background-free search for faint signals.

In the rest of the paper, the known sources of cosmic neutrons are reviewed (section III) after some details of neutron propagation are clarified (section II). Next the interesting energy regions for dark matter particles are reviewed (section IV). Finally, neutron detection techniques are studied, which can be exploited in the search for WIMP decays (section V).

II. PROPAGATION

For a neutron with energy $E = \gamma m_n c^2$, with the neutron mass $m_n = 939.565379(21)$ MeV/ c^2 [2], the time needed to travel the distance x is

$$\Delta t(x) = \frac{x}{v} = \frac{x}{c} \frac{\gamma}{\sqrt{\gamma^2 - 1}} \quad (1)$$

when measured in the observer's reference system, while the corresponding neutron proper time is

$$\tau(x) = \frac{\Delta t(x)}{\gamma} = \frac{x}{c} \frac{1}{\sqrt{\gamma^2 - 1}} \quad (2)$$

assuming that the free neutron is created at the moment of its emission from the source. The life time of a free neutron is τ_0 , hence the survival probability is $P_{\text{surv}}(x) = \exp(-\tau/\tau_0)$, or

$$P_{\text{surv}}(x) = \exp \left[-\frac{x}{c\tau_0 \sqrt{\gamma^2 - 1}} \right] \quad (3)$$

Neglecting interactions (see below), (3) also gives the fraction of monoenergetic neutrons surviving after the

distance x . Unless γ is small, to a good approximation for a source at distance $2x$ one gets the same fraction of surviving neutrons at double energy. If one sets an energy threshold such that, say, $P_{\text{surv}}(x) \geq 0.01$, then this threshold is proportional to x for $\gamma \gg 1$. Similarly, the typical traveled distance for $\gamma \gg 1$ is $\gamma c\tau_0$, which scales linearly with the neutron energy. Thus neutrons at different energies probe different depths, because they cannot come from distances much smaller than $c\tau_0$. In this sense, the knowledge of their direction and energy can be in principle exploited to perform a sort of ‘‘astrotomography’’ of the environment around the observer.

Neutrons propagating in the interstellar medium or through stellar atmospheres may undergo hadronic interactions. The cross-section for n-p interactions on target hydrogen (the most abundant species) is about 1.4 barns at 100 MeV and decreases to a minimum just above 30 mb at 1 GeV, then gently increases up to about 40 mb at 2–3 GeV, remaining at this level up to several hundred GeV (see Figure 49.9 of [2]). Above the minimum, inelastic interactions are the majority, whereas below about 1 GeV one has elastic collisions.

The mean interaction length for neutrons is $\lambda \approx 60$ g cm $^{-2}$ and the probability of no collision $P_{\text{nc}} = \exp[-C\rho x/\lambda]$ has an energy-dependent coefficient C which is proportional to the neutron cross-section. Above 1 GeV, C is a very weak function of the energy, such that P_{nc} only depends on the distance x traveled through the medium with average density ρ . At lower energies one has a rapidly increasing probability of performing elastic collisions. The latter decrease the neutron energy and induce a spread over the initial source direction, with RMS angular dispersion of about $\sqrt{n}6^\circ$, where n is the number of elastic collisions [2]. Hence neutron astronomy is only feasible when the expected number of collisions is smaller than one. This is certainly the case for the propagation through the very low density interstellar medium, as λ is ten times higher than the grammage traversed by charged CR during their *diffusion* in the Galaxy, estimated from the measured ratio of secondary-to-primary nuclei. The actual grammage encountered by neutrons is much smaller than the amount of matter traversed by charged particles, because the former travel along straight lines while the latter are significantly deflected by magnetic fields and perform a random motion inside the Galaxy. Thus, apart from very low energy neutrons (which typically decay before reaching the observer) the expected number of collisions is much smaller than one. In this case the probability of collision $1 - P_{\text{nc}}$ is very small and the fraction of lost neutrons can be well approximated by $C\rho x/\lambda$ (which is very small too, and can be neglected to first approximation).

We can safely assume that inelastic collisions will produce a loss of neutrons, which adds up to the loss due to their beta decay. Because elastic scattering deflect neutrons, a detector pointing toward a point source will most likely miss elastically scattered neutrons even in case of a single collision. Thus we can assume that also

elastic scattering produces a loss of neutrons (those originally traveling along a different direction, which reach the Earth after being deviated in an elastic collision, are ignored). Hence the survival probability is obtained by correcting (3) for the losses due to collisions:

$$P_{\text{surv}}(x) = \exp \left[-\frac{x}{c\tau_0\sqrt{\gamma^2-1}} - \frac{Cx\rho}{\lambda} \right] \quad (4)$$

$$\simeq \exp \left[-\frac{x}{c\tau_0\gamma} - \frac{Cx\rho}{\lambda} \right]$$

where the second expression is valid for $\gamma \gg 1$. This condition is necessary if $x \gg c\tau_0$, in order to have a non negligible $P_{\text{surv}}(x)$ when x is large. In practice the approximation holds whenever neutrons are detected from a source located outside the solar system.

Incidentally, note that the effects of elastic collisions depend on the goal of the analysis. In (4) we consider the propagation through the interstellar medium. However if one is interested into the propagation in the Earth atmosphere then elastic scattering changes the neutron energy but does not decrease their number [3].

Consider the detection at time t of neutrons with energy $E = \gamma m_n c^2$ from a source at distance x , and let $I(\gamma, t; x)$ denote the measured flux in the solid angle $d\Omega$ along the line of sight of the source. The number of measured neutrons in $[\gamma, \gamma + d\gamma]$ and $[t, t + dt]$ is then $N(\gamma, t; x) = I(\gamma, t; x) d\Omega$. The corresponding emitted flux at the source is $I(\gamma, t - \Delta t; 0)$, where the delay Δt is given by (1) as a function of x and γ , and the neutrons emitted by the source in the solid angle $d\Omega$ along the line of sight are given by $N(\gamma, t - \Delta t; 0) = I(\gamma, t - \Delta t; 0) d\Omega$.

Our goal is to estimate $N(\gamma, t - \Delta t; 0)$ from the measurement of $N(\gamma, t; x)$. Once this is achieved, one can get the source term $Q(\gamma, t'; 0) = \frac{4\pi}{d\Omega} N(\gamma, t'; 0)$, which describes the injected spectrum of neutrons as a function of time (denoted t' to keep it different from the measurement time t). The measured number of neutrons is actually given by $N(\gamma, t; x)$ plus the background counts:

$$N(\gamma, t; x) = e^{-\frac{x}{c\tau_0\sqrt{\gamma^2-1}} - \frac{Cx\rho}{\lambda}} N(\gamma, t - \Delta t; 0) + \text{bkg} \quad (5)$$

The latter may be due to instrumental effects, like internal radioactivity of the materials used to build the detector, and to sources of neutrons other than the observed one, like cosmic-ray and atmospheric neutrons. Hence it is important to know this “background” flux as a function of energy.

III. KNOWN SOURCES OF NEUTRONS

We will take the following sources of neutrons into consideration. Three are localized: solar flares, supernova remnants, and a possible giant black hole at the Galaxy center. They can be considered point sources, as even the closest ones, solar flares, have size of 1 arcmin or

less, much smaller than the angular resolution of any conceivable neutron detector at the relevant energies. Two are diffuse sources: neutrons from CR interactions in the Galaxy and in the Earth atmosphere. Localized sources are discussed first.

A. Solar flares

Solar flares are the most powerful events in the solar system, releasing 10^{25} – 10^{26} J in few minutes [4]. A large fraction of this energy, initially stored in magnetic fields in the solar corona, goes into the acceleration of ions and electrons. The latter emit X-rays by bremsstrahlung, hence are directly observable. Indeed, solar flares are the brightest sources of X-rays, with energy ranging from few keV (dominated by thermal emission in the coronal region of the reconnected magnetic flux loop) to several hundreds keV. Above 10–20 keV their distribution is clearly non-thermal, revealing the details of the parent distribution of the accelerated electrons, and is dominated by the footpoints of the magnetic loop, where downward electrons impact on the chromosphere, whose density is about 2 orders of magnitude larger than in the solar corona.

As a consequence of a solar flare, neutrons can be detected on the Earth either as direct emission from the Sun or as secondary products in the atmosphere. Their time signature is clearly different, as the secondary neutrons are produced by the accelerated protons, which reach the Earth only when the latter is magnetically connected to the flaring region. Thus protons need to follow curved magnetic field lines and reach the Earth tens of minutes after the prompt phase of X-ray emission is detected. Entering the Earth atmosphere, they produce showers of secondary particles, including additional neutrons. Solar flares can be detected by the neutron monitors typically located on high mountains, by stratospheric balloon experiments, and by satellite instruments in low Earth orbit.

If neutrons are emitted in the impulsive phase of a solar flare, those with highest energy arrive at the Earth $O(10^3)$ s after their emission (with at most a small delay with respect to X-rays), followed by less energetic neutrons. Their flux should decrease with a typical decay time of $O(10^3)$ s [5]. Hence they are typically well separated in time from the secondary neutrons produced in the hadronic showers induced by the accelerated protons.

During quiet Sun periods, there is no significant direct flux of solar neutrons. Early attempts to measure such a flux date back to the sixties. Hess and Kaifer [6] found no evidence for a diurnal neutron rate variation in 1962, using BF₃ counters on OSO-1 to look for solar neutrons between 10 keV and 10 MeV in a period without solar flares. They have set an upper bound of 2×10^{-3} Hz/cm² on solar neutrons within this energy range, more stringent than the result obtained at the same solar minimum by the Vela satellites [7].

Hess and Kaifer [6] also emphasized that thermonuclear reactions in the solar atmosphere seem to yield a negligibly small neutron flux also in connection with solar flares, concluding that the biggest source of neutrons is from solar protons interacting in the Earth atmosphere.

Direct observations of solar neutrons could only be made two decades later. Chupp *et al.* [8] reported 50–600 MeV neutrons detected at the Earth in correspondence with the solar flare of 1980-06-21 01:18 UT, for about 17 minutes. This measurement was performed by the Gamma-Ray Spectrometer (GRS) flown on the *Solar Maximum Mission* (SMM) and provided evidence for the acceleration of protons up to GeV energies during a solar flare. The peak counting rate was $(3.8 \pm 0.6) \times 10^{-2}$ neutrons/(cm² s) at about 130 MeV. Neutrons have been detected also during the 1980-06-03 11:33 UT flare [9, 10] and during the 1982-06-03 11:43 UT flare [11–13]. This was the first observation of solar neutrons from ground — actually high mountains (Jungfrauoch and Lomnický Stit) — detectors.

The time-dependent neutron flux from a short-duration ($\lesssim 100$ s) solar flare is a sensitive measure of the energy spectrum and number of flare-accelerated protons and nuclei, as shown by Ramaty *et al.* [14]. By looking at the protons from the decay of solar flare neutrons, Evenson *et al.* [15] could determine the spectrum of neutrons emitted during the 1980-06-21 solar flare in the range 10-100 MeV, by solving the diffusion equation under the assumption that neutrons and gamma-rays were generated simultaneously.

Murphy *et al.* [16] emphasized that the same nuclear reactions which produce pions (detected in the gamma-ray range) also produce secondary protons and neutrons. Looking at the gamma-ray and neutron observations from the 1982-06-03 flare, they have built a model based on thick-target interactions, in which nuclear reactions occur as the accelerated particles slow down and stop in the chromosphere. They considered in details the production of neutrons from p-p, p- α and α - α interactions, neglecting heavier nuclei, obtaining a spectrum with a pronounced bump between 500 and 600 MeV. They identified two acceleration phases, with most gamma-rays at 2.223 MeV and 4.1–6.4 MeV emitted during the first one, while the second phase is responsible for most neutrons detected at the Earth.

Neutron monitors on the ground and in the mountains can also detect neutrons emitted from solar flares, although most neutrons are secondary products of solar or galactic CR interactions in the atmosphere. The flux of charged particles depends on the location of the detector, because the Earth magnetic field acts as a shield against soft ions. What matter is the magnetic rigidity $R = pc/(Ze)$, where p is the relativistic momentum and Ze is the ion charge, as it is proportional to the curvature radius $r = R \sin \theta / (Bc)$, where B is the magnetic field intensity and θ is the angle between the ion momentum and the magnetic field. Most published results

provide the CR flux as a function of the kinetic energy

$$E_k = mc^2[\sqrt{1 + (ZeR)^2/(mc^2)^2} - 1] \quad (6)$$

When R is measured in GV, E_k is measured in GeV.

Shea *et al.* [17] reported an increase of neutron rate detected by 7 neutron monitors in USA as a consequence of the solar flare on 1990-05-24 20:46 UT. The detection at stations with geomagnetic cutoff rigidity of about 8 GV was interpreted as a proof that protons have been accelerated at least up to 7 GeV, before they interacted with ions in the solar atmosphere producing neutrons by spallation (a more detailed analysis of the same event is presented by Debrunner *et al.* [18]). In the same solar cycle, Muraki *et al.* [19] reported the detection of 50–360 MeV neutrons associated with the large flare on 1991-06-04 03:37 UT, with a neutron telescope and a muon telescope located at Mount Norikura Cosmic Ray Laboratory at 2770 m above sea level.

The problem with neutron monitors is that they cannot determine whether the neutron is primary or secondary, and they only detect the neutrons after they have undergone collisions in the atmosphere. Hence there is little information about the primary neutron energy. Shibata [3] simulated the propagation of solar neutrons through the Earth atmosphere with Monte Carlo methods, finding that elastic scattering plays an important role at neutron energies below 200 MeV.

Another way of detecting solar neutrons is to focus on the enhancement of protons and electrons resulting from their beta decay. During solar cycle 23, looking at protons and electrons measured by the 3DP experiment on board the *Wind* spacecraft, Agueda *et al.* [20] obtained the spectrum of 1–10 MeV solar neutrons. They found that the neutron spectrum escaping the Sun is well below the observed background proton spectrum. At these energies, most neutrons decay before reaching the Earth. Future missions such *Solar Probe* and *Solar Orbiter* will operate at radial distances < 1 AU, where the neutron flux is higher (about 65% of 10 MeV neutrons decay before reaching 0.3 AU, the perihelion distance of these missions) and is potentially detectable.

The SONG instrument onboard CORONAS-F detected neutrons and gamma-rays in four events, on 26, 28, and 29 October and on 4 November 2003. The 2003-10-28 flare was the best observation, as reported by Kuznetsov *et al.* [21].

More recently, Muraki *et al.* [22] reported the simultaneous observation of solar neutrons from the SEDA-NEM instrument on board the International Space Station [23] and high mountain observatories located in Mt. Chacaltaya, Bolivia, and Mt. Sierra Negra, Mexico, associated with the flare 2014-07-08 16:06 UT.

Finally, a dozen flares are associated with detected neutron fluxes at the Earth, with space and/or ground observations. They are considered in details by Yu *et al.* [24], where also the theoretical aspects are reviewed.

B. Galaxy center

Solar flares inject neutrons in the interplanetary space with energies up to the GeV range and in well defined time intervals. On the other extreme of the CR energy spectrum, at the so-called CR ankle, there is indirect evidence of neutrons coming from a region close to the Galaxy center with energies of order of 10^{18} eV.

At these energies, measurements can only be performed by looking at atmospheric showers, hence it is impossible to distinguish a neutron-initiated cascade from a proton event. However, the distribution of ultra high energy CR shows a small anisotropy which is not detected at lower energies. Such anisotropy was first reported by the AGASA air shower array at 4% level around 10^{18} eV, and it was interpreted as an excess near the directions of the Galactic Center and the Cygnus region [25]. More recently, the Pierre Auger Observatory has also confirmed the presence of this anisotropy at 4.4% level (amplitude of first harmonic) [26].

Such an excess is most easily explained in terms of neutral particles, which travel along the line of sight of their source. The Galaxy center is 7.6–8.7 kpc away, hence the range of γ is $(8.8\text{--}10.0)\times 10^8$, which corresponds to a neutron energy $E = (8.3\text{--}9.5)\times 10^{17}$ eV. Hence neutrons from this region, if any, can only contribute to the ankle portion of the CR spectrum. Clay [27] interpreted the anisotropy reported by AGASA as an evidence for a detection of 10^{18} eV neutrons, because protons would not travel along straight lines.

In the CR spectrum between 10^{18} and 10^{20} eV there are two changes of slope, with a flux increase around 8.5×10^{18} eV and a steep decrease above 4×10^{19} eV (see e.g. Figure 29.8 of [2]). The hardening of the spectrum around 8.5×10^{18} eV is remarkably close to the neutron energy threshold of $8.4\text{--}8.7 \times 10^{17}$ eV inferred from the distance of 7860 ± 140 pc of Sagittarius A*, where a supermassive black hole with relativistic jets is located [28]. If this were the only active source in this energy region (which is likely not the case), one could think that the steepening above 4×10^{19} eV reflects the true neutron spectrum (e.g. the spectral index and the normalization of a power-law model), because at these energies most neutrons reach the Earth without decaying. This is not in agreement with the “classical” explanation of the ankle as the region where there is a transition between a galactic component and an extragalactic contribution. On the other hand, it is not straightforward to explain all measured details of the ultra high energy cosmic ray spectrum in terms of this transition (for a recent discussion, see e.g. [29]). Hence it is not excluded that a neutron component may affect the energy spectrum, in addition to providing a simple explanation for the detected anisotropy.

Cygnus X-1 is a black hole X-ray binary located at 2200 ± 200 pc, emitting gamma-rays with energies in excess of 100 GeV [30]. It can contribute neutrons above 2×10^{17} eV, at the so-called second knee of the CR spectrum. Of course, any source of high-energy neutrons is

expected to emit also protons (and other charged particles). However, protons diffuse for millions of years in the Galaxy before reaching the Earth, contributing to the CR spectrum with a long delay with respect to neutrons, which travel straight practically at the speed of light. Thus neutrons from Cygnus X-1 take about 6500 years to reach the Earth, while those from Sagittarius A* take about 25600 years, both arriving much before the protons ejected at the same time at the source can be detected.

Although it is suggestive that the energy thresholds connected to Cygnus X-1 and Sagittarius A* correspond to known features of the CR spectrum, one should not forget that there may be additional sources, likely of galactic origin below the ankle and extragalactic in the ankle region.

On the other hand, also these source can emit neutrons, which play an important astrophysical role. For example, Sikora *et al.* [31] considered the creation of relativistic neutrons in active galactic nuclei (AGN). They are an efficient way of transporting a fraction of the total energy output away from the AGN, thanks to their big interaction length. Their decays then release this energy after 1–100 pc, producing charged particles (protons and electrons), which interact almost locally, and neutrinos. Furthermore, Tkaczyk [32] concluded that about half of the AGN acceleration power is transferred to relativistic neutrons, which can then escape the region of strong magnetic field. This makes it possible to transfer a large amount of mass and energy in hadronic jets. The photodisintegration process of the nucleus is a powerful source of neutrons, because the photodisintegration time of nuclei in comparison to the photopion production time is an order of magnitude shorter, and so the nuclei are completely destroyed first. On average, a nucleus with mass number A generates half of its own mass in neutrons with the same Lorentz factor.

C. Supernova remnants

Neutrons emitted during solar flares have been detected in several events, and there is indirect evidence for a neutron component causing the observed anisotropy in the ultra high energy CR spectrum. Supernova remnants (SNR) should also provide a detectable flux of neutrons, but this remained undetected so far.

The SNR distances range from 150 ly to 39000 ly [33][34], i.e. from $5.3 \times 10^6 c\tau_0$ to $1.4 \times 10^9 c\tau_0$. Hence the energy threshold varies from 5.0×10^{15} eV to 1.3×10^{18} eV, i.e. it spans the region of the CR spectrum encompassing the knee and the second knee, where the measured CR spectrum (with air shower detectors) shows a few changes in slope (see Figure 29.8 of [2]). The distribution of the logarithm of the SNR distance (figure 1) is slightly asymmetric, with a broad peak close to 8.5, which corresponds to an energy scale of about 3×10^{17} eV. The median is 8.24, corresponding to $E = 1.6 \times 10^{17}$ eV. At these ener-

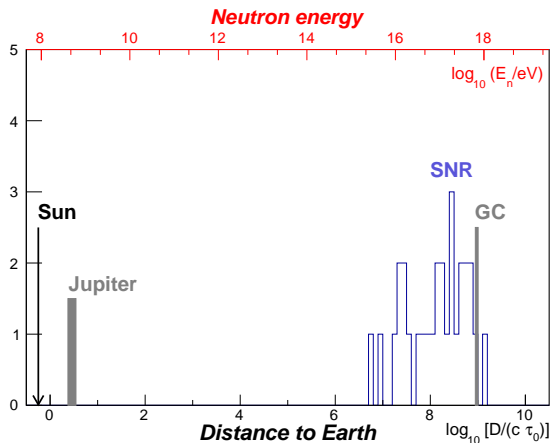


FIG. 1. Distance of identified progenitors of supernova remnants, compared to other astrophysical objects: the Sun (at 1 AU), Jupiter (at variable distance of 4.2-6.2 AU from the Earth), and the Galactic Center (whose distance is uncertain). The typical neutron energy in eV is shown by the red scale.

gies, the CR spectrum has a feature called second knee. The 0.25-quantile corresponds to 3.7×10^{17} eV, just above the slope change between the knee and the second knee. Finally, the 0.75-quantile corresponds to 4.0×10^{17} eV, a region in which a single power-law seems to correctly model the CR energy spectrum up to the ankle.

Together with the correspondence between the ankle and the threshold energy for neutrons coming from the Galaxy center, the energy scales related to the SNR distances are suggestive of a non coincidental connection with the shape of the CR spectrum at very high energies. Apart from the long time delay between the arrival of neutral and charged particles to the Earth, the problem is that in this energy region there is no way of identifying the parent particle, which gives rise to the hadronic cascade in the Earth atmosphere. The author is not aware of any simulation, in which ions and neutrons are emitted from several point sources corresponding to the known supernova remnants, and are traced inside the Galaxy until they reach the Earth. However, the absence of a significant anisotropy below the ankle implies that free neutrons cannot be a large fraction of the detected particles.

D. Cosmic neutrons

In the wide energy range from solar flares to supernova remnants, there is no known point source of neutrons, which can reach the Earth before decaying. Thus, one is left with the diffuse background of secondary cosmic neutrons produced by the interactions of cosmic rays with the interstellar medium and with those produced in the stellar and planetary atmospheres. The flux of the diffuse component of cosmic neutrons was never detected so far, and at low energies is much smaller than the albedo

component due to CR initiated hadronic showers in the Earth atmosphere (discussed below in section III E).

As an order of magnitude estimate for the diffuse cosmic neutron flux, one can take the CR antiproton flux, recently measured by PAMELA [35] and AMS-02 [36] from 60 MeV up to few hundred GeV. The simplest process with production of antiprotons is the collision of a CR proton with a hydrogen atom of the interstellar medium: $p + p \rightarrow p + p + p + \bar{p}$. The energy threshold (1.88 GeV in the center of momentum system) is higher than the threshold (1.08 GeV) for the simpler reaction with a secondary neutron in the final state, $p + p \rightarrow p + n + \pi^+$. This means that the low-energy region is a bit harder for the neutrons than for the antiprotons, although it does not make any sizable difference at high energies.

The number density of secondary antiprotons provides a lower bound on secondary neutrons, because free neutrons can also be produced by spallation, as fragments of larger nuclei which act as targets for CR protons. However, spallation is not expected to inflate significantly the number density of free neutrons, because elements heavier than hydrogen are present only in small amounts: the number density of He is only about 10% of H, and the sum of O, Ne, N and C (the next most abundant species in the universe) is about 0.1% of the hydrogen density.

On the other hand, the flux of charged particles can be significantly different from the flux of neutral particles with the same number density. The reason is magnetic deflection: while a neutral particle travels along a straight path and has only one chance to cross a detector, a charged particle may be deflected by the magnetic field and cross more than once a given surface. This effect is evident for the trapped protons and electrons in the Earth magnetosphere (an effect known since decades, and measured with unprecedented precision by AMS-01 [37, 38] and PAMELA [39–41]), and should work similarly over wide regions if the magnetic field intensity is smaller. Thus, the measured flux of charged particle is enhanced by any sort of trapping, whereas the flux of neutral particles is independent of magnetic fields. However, at present is not known by how much the charged particle flux in the solar system is enhanced.

One further complication with neutrons is that they may be also created by electron capture from protons and electrons trapped in the same region. This is suggested by the comparison between the neutron measurements in the Van Allen belts by the Russian missions *Salut-7* and *Kosmos-1686* [42] and the earlier measurements by COMPTTEL [43] and several balloon flights (more details in section III E), which all agree on neutron fluxes smaller by one order of magnitude.

If the size of the trapping region (which has to be not too far from the solar system) is not much bigger than $\gamma c \tau_0$, then the flux of neutrons with Lorentz factor γ is enhanced, where γ is of the same order of magnitude of the proton and electron Lorentz factors. On the other hand, the larger is γ the larger is the rigidity R of the parent charged particles, hence the larger is the curvature

radius $r \simeq R/(Bc)$ for a given magnetic field intensity B . For a proton with rigidity of 1 GV in a region with field intensity of 1 μG , the curvature radius is 10^{-5} pc, of the same order of magnitude as $c\tau_0$. The same field will trap protons and electrons of 10 GV in a region with linear size comparable to $10c\tau_0$, where neutrons with $\gamma \approx 10$ may be created by electron capture. Hence in the simplest model in which the neutron Lorentz factor is the same as that of the parent proton and electron, one has neutronization happening over distances which are of the order of the neutron decay length at all momenta below some critical limit, above which the number of protons and electrons escaping from the region becomes important. So below this limit, the enhancement of the secondary neutron flux is almost independent of γ .

In absence of a detailed simulation of the neutral and charged CR flux in our galactic environment, we take the CR antiproton flux as a first estimate of the neutron flux. The antiproton flux measured by PAMELA increases from about $7 \times 10^{-3} (\text{m}^2 \text{sr s GeV})^{-1}$ between 50 and 100 MeV, to $27 \times 10^{-3} (\text{m}^2 \text{sr s GeV})^{-1}$ between 2.6 and 3.0 GeV, then decreases at the level of $5 \times 10^{-3} (\text{m}^2 \text{sr s GeV})^{-1}$ at 10 GeV, $7 \times 10^{-4} (\text{m}^2 \text{sr s GeV})^{-1}$ at 20 GeV, down to $2 \times 10^{-5} (\text{m}^2 \text{sr s GeV})^{-1}$ above 50 GeV [35]. The measurement by AMS-02 gives an antiproton flux reaching a maximum of about $1.7 \times 10^{-2} (\text{m}^2 \text{sr s GeV})^{-1}$ at 3 GeV, consistent with the PAMELA result within the uncertainties, decreasing by a factor of 10 at 16 GeV, by another factor of 10 at 35 GeV, by another factor of 10 at 80 GeV, by another factor of 10 at 200 GeV, until reaching $2 \times 10^{-7} (\text{m}^2 \text{sr s GeV})^{-1}$ between 260 and 450 GeV [36].

At rigidities high enough that the solar modulation can be neglected, the antiproton to proton ratio is almost constant, just below 2×10^{-4} . This means that a neutron detector in space must achieve a separation power of at least 10^{-5} between neutrons and protons, which should be feasible because the latter can be very efficiently vetoed by surrounding the detector with an anticoincidence scintillating layer.

E. Atmospheric neutrons

A detectable flux of secondary neutrons is produced by CR-induced hadronic showers in the Earth atmosphere, which provide a steady state source with slow time variations connected to the solar activity. Secondary neutrons may be detected promptly or after they have lost most of their initial energy in elastic collisions with the air molecules. At low energy, thermalized neutrons can be captured by atoms, which de-excite by emitting gamma-rays. The absorption (n, γ) process contributes up to few tens keV, as noticed by Hess *et al.* [44], who measured the neutron spectrum from 0.01 eV to 10 GeV in the Earth atmosphere with a series of balloon experiments in the fifties. Below 10 keV the neutron flux scales roughly as $1/E$, as it would be expected in an infinite nonabsorb-

ing medium in which neutrons slow down by collisions with an energy-independent cross-section. They found that the main deviation from $1/E$ arises from the energy dependence of the cross section, which flattens a bit the spectrum, giving a flux proportional to $E^{-0.88}$ from about 1 eV to 50 keV. Below 1 eV neutron absorption by nitrogen is an important process, competing with thermalization, and the flux is damped. At 1 MeV the shape is affected by the source contribution of “nuclear evaporation” process, producing a bump with a very broad peak at about 500 keV. Beyond this bump, the spectrum falls down approximately as $1/E$, becoming softer above ~ 100 MeV.

Eyles *et al.* [45] measured the neutron “albedo” between 50 and 350 MeV with balloon flights between 1967 and 1970, and found no evidence for a primary flux of neutrons. Other measurements have been performed more or less in the same period e.g. by Preszler *et al.* [46] and Kanbach *et al.* [47], confirmed later on by the COMPTEL gamma-ray instrument on board of *CGRO* [43].

Using data from the Russian missions *Salut-7* and *Kosmos-1686*, Bogomolov *et al.* [42] measured the neutron flux under the Earth radiation belts with a rigidity cutoff of 4.5 GV, finding a spectrum with shape similar as (but not identical to) the previous measurements, but almost one order of magnitude more intense than the measurements reported above. Unless this is due to some systematic uncertainty in the absolute calibration, this result would imply that the electron capture reaction from the protons and electrons trapped in the Van Allen belts enhances the flux of neutrons.

Neutron flux measurements have been also performed in order to estimate the radiation effects on airline crews and astronauts. In particular, Badhwar *et al.* [48] measured the 1–14 MeV neutrons onboard the NASA space shuttle during the STS-31 mission, whereas Matsumoto *et al.* [49] performed a measurement during the STS-89 space shuttle mission from thermal energies up to 100 MeV, confirming that the neutron flux depends on the amount of trapped low-energy particles. The measured neutron rates in the equatorial region (about 0.2 Hz/cm² at 1 MeV) are about 5 times smaller than in the polar region (1 Hz/cm² at 1 MeV), which in turn is smaller than in the South Atlantic Anomaly (5 Hz/cm² at 1 MeV). Later, Koshiishi *et al.* [50] published the orbit-averaged neutron spectra up to 100 MeV, obtained on the International Space Station while orbiting in different geomagnetic regions from March to November 2001. The shape is similar to what is reported by Matsumoto *et al.* [49] and the normalization is in between the equatorial and polar regions, as expected.

In order to provide an estimate of the neutron flux at the top of the atmosphere, we quote here few values: about 1 kHz/(m² MeV) at 1 MeV and 0.1 kHz/(m² MeV) at 10 MeV [44, 51], 20–30 Hz/(m² MeV) at 50 MeV [44, 51, 52], about 8 Hz/(m² MeV) at 100 MeV and 0.7 Hz/(m² MeV) at 300 MeV [52]. The rate becomes about

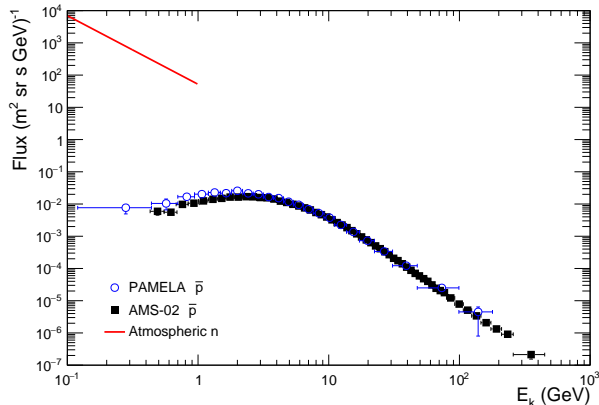


FIG. 2. Comparison between albedo neutrons (continuous line) and antiproton flux. The flux of atmospheric neutrons is a power-law with spectral index 2.13 [52]. Data points represent PAMELA [35] and AMS-02 [36] antiproton measurements.

10 times higher inside the geomagnetic belts, where the soft trapped protons and electrons may give birth to neutrons via electron capture. In the same energy region, from time to time neutrons from solar flares dominate the rate for a relatively short duration. Anyway, even in quite Sun periods at low energy — measurements are available only up to few hundred MeV — the secondary neutrons produced in the Earth atmosphere are many more than the expected diffuse cosmic neutron flux (figure 2), hence it is fundamental to be able to separate these two components.

For a detector orbiting outside the Earth atmosphere, secondary neutrons mostly comes from below (hence the name “albedo neutrons”), with a flux which is expected to be sizable up to the tangential direction and decrease significantly when looking upward. This means that the background from albedo neutrons can be suppressed using a directional detector, or by performing a differential measurement comparing zenith and nadir fluxes.

The Earth magnetic field affects the flux of incoming charged particles, reflecting low-energy particles as a function of their magnetic rigidity. Hence the neutron spectrum was studied by Morris *et al.* [43] as a function of the geomagnetic cutoff and of the geocentric zenith angle. The measurement is well fitted by the product of an exponential term in cut-off rigidity, a linear function of the zenith angle (ranging from 3° to 177°), and a factor accounting for the solar modulation. The linear dependence on the zenith angle is attributed to the screening of the *CGRO* spacecraft mass, which is much more important than the production of secondary neutrons in the spacecraft itself. Later, Morris *et al.* [52] reanalyzed the same COMPTEL data and fitted them together with previous measurements, obtaining a broken power-law with spectral indices of 0.56 below 67 MeV and 2.13 above this energy. The normalization is found to depend on

the Mount Washington neutron monitor rate.

IV. DARK MATTER SEARCHES

As we have seen, solar flares are the only known astrophysical source of neutrons, which have been detected so far. Solar neutrons may reach the Earth from about 20 MeV (below which they mostly decay in flight [53]) to few GeV (above which the injected flux becomes negligible), with a tight time correlation with X-ray flares. Hence solar flare neutrons are easily identifiable events.

If an instrument in orbit is able to recognize secondary neutrons produced by CR interactions in the Earth atmosphere, what remains is a very low cosmic neutron flux, which so far remained undetected, spanning a wide energy range up to the CR knee region, above which supernova remnants are expected to contribute (however, at these energies one cannot identify the incoming particle and the only possibility is to perform statistical studies of the hadronic showers produced in the atmosphere).

Thus, the diffuse cosmic neutron flux is a (very low) background for searches for exotic signatures, like the final products of the annihilation of dark matter (DM) particles. Hence it is interesting to know which energy regions are best suitable for DM searches with a neutron detector in space.

The chapter on DM searches of the latest Review of Particle Physics [2] lists a number of candidates, like primordial black holes, axions, sterile neutrinos, and weakly interacting massive particles (WIMPs). Among them, primordial black holes are not directly detectable, although their accretion jets may well emit neutrons with a wide energy range, as we mentioned about AGNs in section III B. Thus they are not considered in this section. The mass range for axions is within the thermal range for neutrons, at which neutron capture takes place. The albedo component is overwhelming in this case, because there is no directional detection, hence axions are not considered in the following. Sterile neutrinos with keV masses are invisible for an orbital detector: even in case one could detect a nuclear recoil from such a low energy particles, the sensitive volume would need to be enormous because of the extremely small neutrino cross-section. So we are left with WIMPs, which are the most promising candidates for the “cold DM models” which best fit all available astrophysical and cosmological data (see [2] and references therein). WIMPs masses may range from about 10 GeV to few TeV, which is the energy range in which the cosmic neutron background is very low. Lighter candidates have been also proposed, like strongly interacting massive particles (SIMPs) with masses in the MeV to GeV range [54]. They may also annihilate in fermion-antifermion pairs, like WIMPs.

The current approach for indirect detection of DM particles with masses from MeV to TeV is to look for a “bump” in the cosmic gamma, positron and antiproton fluxes, as currently being done by different space experi-

ments. However, the same decays that create antiproton-proton pairs will also create antineutron-neutron pairs. Hence, one may also measure the cosmic neutron flux and look for an excess in some energy range. The advantage of this approach is that neutrons provide directional information. For example, massive objects like the Sun or Jupiter may attract DM particles increasing their local density, and so also their interaction rate. Thus, an excess of neutrons coming from the Sun in periods without solar flares could be interpreted in terms of local DM density.

Note that [55] obtained a DM density of 0.43 ± 0.15 GeV/cm³ in the galactic region of the solar system, a bit higher than the galactic average commonly used in the literature (0.3 GeV/cm³). However this does not account for the presence of compact massive objects like the Sun. Indeed, the gravitational field of the Sun may locally enhance the DM density by orders of magnitude. However, any uncertainty on the galactic DM density is also amplified the same way, making an estimate of the density around the Earth unfeasible [56].

Among the direct detection attempts [57], there is a positive measurement claimed by the DAMA/LIBRA collaboration [58, 59], who found an annual modulation with the expected period (1 year) and phase (maximum around June 2) for a distribution of DM particles crossed by the solar system, with the Earth moving forward or backward with respect to the Sun motion every 6 months. Interpreted in terms of WIMPs, two scenarios appear most plausible: a 50 GeV mass with cross-section of 7×10^{-6} pb or a particle with mass of 6–10 GeV and cross-section of order 10^{-3} pb [2]. However, this result was criticized and could not be reproduced by other direct-detection experiments, which instead rejected the signal claimed by DAMA/LIBRA. Nevertheless, the annual modulation detected by DAMA and LIBRA could not be explained by some other mechanism so far. Hence these mass regions remain interesting.

Other (debated) positive results have been also claimed by other experiments. CRESST found a signal compatible with WIMP masses of about 11 GeV or 22 GeV [60]. CDMS found a signal compatible with a WIMP mass of about 10 GeV [61]. CoGeNT also found some evidence for an annual modulation compatible with a WIMP mass of 7 GeV [62].

Note that radio observations of the Ursa Major II dwarf spheroidal galaxy [63], interpreted in terms of possible DM annihilation into e^+e^- producing synchrotron radiation in the magnetic field of the dwarf galaxy, exclude 10 GeV WIMP for $B > 0.6$ μ G at the thermal rate $\langle\sigma v\rangle = 2.18 \times 10^{-26}$ cm³/s at 2σ level. However, they do not constrain decays into other fermion pairs.

On the side of indirect detection, interesting results emerge both from gamma-ray and from cosmic-ray measurements. *Fermi*-LAT data show an excess of GeV photons from an extended region around the Galaxy center [64, 65]. Explanations in terms of standard objects, like a population of thousands unresolved millisecond pulsars,

might be able to explain the emission from the Galactic Center, but are challenged by the fact that the signal extends well beyond the boundaries of the central stellar cluster [65]. On the other hand, models with DM particles of 7–10 GeV, which annihilate primarily into a $\tau^+\tau^-$ final state but also into hadronic final states, well reproduce the data. However, Daylan *et al.* [65] emphasize that better fits are obtained with heavier particles (with masses in the range 20–60 GeV) annihilating mostly into quarks. These mass ranges are remarkably similar to those preferred by DAMA/LIBRA.

Another interesting result is the excess of photons around 130 GeV discovered in 2012 using public *Fermi*-LAT data [66] but no longer visible in a reanalysis of the same data [67] and also excluded by H.E.S.S. [68]. Interestingly, WMAP data have been also interpreted as evidence for annihilation of WIMPs with masses above 100 GeV [69], however there is no consensus on this [70].

Finally, the CR electron and positron measurements also reveal interesting details. The positron fraction measured by PAMELA [71] and AMS-02 [72] increases between 10 and 200 GeV, and then flattens above 200 GeV. The behavior of the positron fraction, considered together with the rather hard electron spectrum measured by PAMELA [73], AMS-02 [74] ATIC [75], *Fermi*-LAT [76] and H.E.S.S. [77] between 100 and 1000 GeV, can in principle be explained through WIMP annihilation. However, it is likely that nearby and recent supernova or pulsar sources of electrons and positrons can also explain the observed features.

WIMP annihilations would also produce detectable features in the antiproton and antideuteron spectra [78]. Using the latest AMS-02 antiproton measurement, two independent groups [79, 80] claimed that a dark matter signal with mass between 20 and 80 GeV and velocity-averaged hadronic annihilation cross-section of order 10^{-26} cm³s⁻¹ is able to reproduce the data much better than the background-only hypothesis. While the analysis in [80] has a net preference for masses of about 70–80 GeV and $\langle\sigma v\rangle \approx 3 \times 10^{-26}$ cm³/s, [79] obtain a more diagonal contour map extending to lower masses and velocity-averaged cross-sections, with a more pronounced dependence on the parametrization of the antiproton production cross-section.

This suggests that some signature should also be visible in the neutron spectrum, at the same energies. However, neutrons have shorter range than electrons and positrons, hence probe a small portion of the Galaxy around the solar system. For example, 80 GeV neutrons come mostly from a sphere of radius 142 AU (a bit larger than the solar system), while positrons come from distances bigger than 1 kp (of order of the thickness of the galactic disk) [81]. Both sample a much smaller region than protons and He nuclei, diffusing for tens of millions years in a large fraction of the Galaxy.

A lower limit to the DM contribution to the local neutron flux can be obtained from the galactic averaged DM density. For example, 80 GeV neutrons might

come from the annihilation of ~ 80 GeV WIMPs, whose galactic-averaged number density n_{80} would be about 0.005 cm^{-3} . The annihilation rate would be $\Gamma_{80} = \frac{1}{2}n_{80}^2\langle\sigma v\rangle$ which, using $\langle\sigma v\rangle = 3 \times 10^{-26} \text{ cm}^3/\text{s}$, gives $\Gamma_{80} = 3.8 \times 10^{-31} \text{ cm}^{-3} \text{ s}^{-1}$. We are only interested into annihilations happening inside a sphere with radius $\gamma c\tau_0 = 2.1 \times 10^{15} \text{ cm}$, that is inside a volume $V = 4 \times 10^{46} \text{ cm}^3$. The annihilation rate inside this volume is $\Gamma V = 1.5 \times 10^{16} \text{ s}^{-1}$ and, to first approximation, this is also the production rate of neutrons. As neutrons decay in the lab-frame after $\gamma\tau_0 = 7 \times 10^4 \text{ s}$, DM annihilations provide a stationary neutron population inside V with density $N/V = \Gamma\gamma\tau_0 = 2.5 \times 10^{-26} \text{ cm}^{-3}$. These neutrons have a homogeneous and isotropic distribution of particles traveling at the speed of light. A given flat surface A (say the entrance face of a detector) is reachable by all neutrons contained in a hemisphere centered on A with radius $\gamma c\tau_0$. The rate at which they cross A is $r = 2\pi\gamma cAN/V$. If $A = 1 \text{ m}^2$, $r = 3.8 \times 10^{-10} \text{ s}^{-1}$, which is extremely low. This lower limit applies in the interstellar space, far from the gravitational influence of star-like bodies. However around the Earth the DM density should be much higher than the galactic average because of the Sun gravitational field. Hence it is well possible that the local rate is several orders of magnitude bigger [56].

In addition to the amplification of the DM signal close to star-like objects mentioned above, there is another interesting mechanism that can increase the neutron flux from DM, not by incrementing the DM density but by extending enormously the sampled volume. This is the DM “transporting” mechanism, which [82] invoke to reconcile the positron measurements with antiproton data. As mentioned above, positrons and electrons probe a volume considerably smaller than protons and antiprotons. Hence positron data, interpreted in terms of a DM source, imply a too large cross-section or density compared to computations performed with average galactic values, which reproduce antiproton data. However, the two types of measurements can be reconciled in case DM annihilations, happening mostly in the central region of the Galaxy, produce an unstable intermediate dark-sector state, which subsequently decays into a lighter DM particle in the vicinity of the Earth.

Although the specific model presented in [82] does not enhance the local neutron flux, because it is based on a dark-sector state which pairs preferentially to leptons, the authors confirm that the same theoretical approach can work as well if light quarks are produced in the decay of the intermediate state. In particular, the accessible volume increases proportionally to the decay range of the dark-sector particle, which depends on the mass difference between the heavier DM particle and the invisible carrier. As the accessible volume scales as the third power of the Lorentz factor, an invisible carrier which is significantly lighter than the progenitor DM particle extends the volume contributing to the local flux of neutrons by few orders of magnitude. In this model low-

energy neutrons may derive from DM annihilations in distant regions, because the actual neutron production happens close to the detector. In addition, one may get relatively soft neutrons (say below 10 GeV) also from a heavy DM particle (say above 100 GeV), depending on the mass of the intermediate invisible state and its decay.

In summary, neutrons are created by the same reactions that produce antiprotons, including possible WIMP annihilations or decays. Contrary to antiprotons and positrons, neutrons provide directional information, which is unavailable with charged particles. Although neutrons may come from a limited volume, in the energy range which is relevant for DM searches there is no other “background” source of neutrons. Thus, any detection of cosmic neutrons with a precise energy signature would be a smoking gun pointing toward the existence of new particles.

V. NEUTRON DETECTION

The most interesting mass range for WIMPs goes from few GeV to few hundred GeV. Hence the ideal neutron detector should have the following characteristics. First, it should operate in an energy range which covers the solar flare emissions at the low-energy side, and reach the highest possible range (ideally up to the TeV scale, but this is hardly possible). Second, it should possess directional capability, in order to locate the source of each neutron. Third, it should operate in space, such that the atmospheric neutrons have a well defined directional distribution, and can be separated from the other sources, including the diffuse cosmic neutron background. Fourth, it should have an excellent rejection power for charged cosmic rays, and allow for pulse-shape discrimination to efficiently separate gamma rays from neutrons. Finally, it should have sufficiently good energy resolution to provide an estimate of the WIMP mass in case of the detection of an excess over the background.

Of course, achieving all this goals at the same time is quite difficult, if not impossible. The main challenge is represented by the trade between the energy range, the detector size, and the directionality. Although it is desirable to reach very high energies in order to probe the WIMP parameter space up to few hundred GeV mass, the expected neutron flux is a falling function of the energy and the counting rate becomes quickly negligible unless the effective area is very large. A 4π geometry has the largest effective area, but it is difficult to reconcile with the need of reconstructing the incoming neutron direction. For example, Pioch *et al.* [83] showed that a Bonner sphere spectrometer provides sensitivity up to 100 GeV, but this kind of detector does not provide information about the incoming direction, because neutrons must be thermalized before being detected. A directional neutron detector with large effective area, which is able to measure high energies, must necessarily be a large-volume heavy-material instrument. As such, it is very

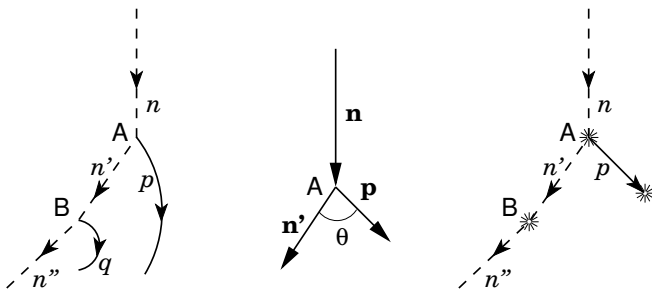


FIG. 3. Incoming neutron with 4-momentum n and 3-momentum \mathbf{n} undergoing two collisions in the detector active volume. Left: particles trajectories in a magnetic spectrometer. Center: 3-momenta configuration at the first elastic collision. Right: calorimeter view of the same pair of collisions.

hard to put it in orbit. Whereas at low energies (up to few GeV) the n-p elastic scattering can be exploited to reconstruct the initial neutron momentum (see below), at high energies inelastic scattering dominates and hadronic showers are produced. By reconstructing the shape of the shower, one may find the initial direction and the total neutron energy, but hadronic cascades develop over wide volumes and total containment requires a very large detector. At the same time, one should choose an active material which possesses heavy nuclei, to increase the interaction probability, which again goes toward larger detector masses. The alternative is to build a sampling calorimeter, in which the active material can be plastic scintillator, but the final result is still very massive, because of the required layers of heavy material that are needed to improve the development of a hadronic cascade.

A. Kinematics of elastic scattering

Assume that the neutron undergoes two interactions in the detector volume, and that the first is an elastic interaction in which a hydrogen nucleus (considered as a free proton) is kicked out of a molecule. The best active medium for the first scattering is thus an organic scintillator. Let n, n', p represent the 4-momenta of the neutron before and after the first collision, and the 4-momentum of the proton emitted in the first elastic scattering, respectively. Next, assume that the scattered neutron interacts a second time inside the detector. Finally, assume that the detector is able to measure the positions A and B of the first and second neutron collisions and the 4-momentum of the proton scattered at point A.

Figure 3 shows two possibilities for neutron detection, in the case of a magnetic spectrometer (left) and with a sampling calorimeter (right). In both cases, it is assumed that the 3D positions of the two scattering sites A and B are measured together with the 4-momentum of the proton kicked off by the first collision. In the case of a

magnetic spectrometer, the 3-momentum \mathbf{p} of the proton is measured, whereas its total energy E_p and direction are measured by the calorimeter. The proton is identified by looking at the details of its energy loss and velocity, and the 4-momentum is reconstructed by assuming that the visible particle has the proton mass m_p making use of the relation $p^2 = m_p^2 = E_p^2 - \mathbf{p}^2$ (using units $c = 1$ in this section).

Conservation of 4-momentum reads $n = n' + p$ and the direction of the neutron after the first interaction is known from the two position measurements. In order to find the initial 4-momentum n we need first to find the magnitude of n' . This is obtained by taking the square of the 4-momentum conservation law, which gives relativistic invariants on both sides of the equation: $n^2 = (n' + p)^2$ gives

$$m_n^2 = m_n^2 + m_p^2 + 2(E_p E_{n'} - |\mathbf{p}| |\mathbf{n}'| \cos \theta) \quad (7)$$

from which one finds the magnitude of the scattered neutron 3-momentum:

$$|\mathbf{n}'| = \frac{m_p^2}{2p_L} + E_{n'} \frac{E_p}{p_L} \quad (8)$$

where the longitudinal momentum $p_L = |\mathbf{p}| \cos \theta$ is the measured component of the proton 3-momentum \mathbf{p} along the direction AB of the scattered neutron.

The only unknown quantity in the right hand side of (8) is the energy $E_{n'}$ of the scattered neutron. By substituting $E_{n'} = \gamma m_n$ and $|\mathbf{n}'| = \sqrt{\gamma^2 - 1} m_n$ in equation (8), one obtains a quadratic equation for the Lorentz factor γ of the scattered neutron

$$\left(\frac{E_p^2}{p_L^2} - 1 \right) \gamma^2 + \frac{m_p^2 E_p}{m_n p_L^2} \gamma + \frac{m_p^4}{4m_n^2 p_L^2} + 1 = 0 \quad (9)$$

with two formal roots, although the presence of measurement uncertainties forces one to employ numerical methods to find its optimal solution. Together with the direction $AB = \hat{\mathbf{n}}'$, the solution γ of equation (9) gives the 3-momentum of the scattered neutron, $\mathbf{n}' = \sqrt{\gamma^2 - 1} m_n \hat{\mathbf{n}}'$, from which one finds the 3-momentum \mathbf{n} of the incoming neutron:

$$\mathbf{n} = \mathbf{n}' + \mathbf{p} = \sqrt{\gamma^2 - 1} m_n \hat{\mathbf{n}}' + \mathbf{p}. \quad (10)$$

Thus (10) gives the direction of the source and allows us to obtain the energy of the input neutron from the relation $E_n^2 = m_n^2 + \mathbf{n}^2$.

If the total energy of the scattered neutron is also measured in the second collision, one gets a better estimate of the incoming neutron energy. The best way to measure the total energy is to adopt a hadronic calorimeter as a second detection stage, because this will also work for events in which there is no elastic collision in the first place.

B. Detector design

Although no study on neutron detection has been published by the AMS collaboration, it is hopefully possible to select n-p elastic scatterings in the transition radiation detection (TRD) system of AMS-02 by selecting events in which a single proton track starts inside the TRD (i.e. by using the first TRD layers in anticoincidence) and crosses the triggering scintillators of the time of flight system. However, this only works if the efficiency of the first TRD layers is close to 100% (which sounds unlikely), because proton events are about 10^4 times more frequent than neutrons. In addition, it is difficult to detect also the second neutron interaction inside AMS-02, although this is perhaps possible by tuning the selection criteria (this event topology would be discarded as “noise” in the standard CR selection). The electromagnetic calorimeter of AMS-02 can detect gamma-rays, and might have a small but non negligible efficiency also for neutrons. However, no study has been published about them yet. Hence at best AMS-02 has a very small acceptance for neutron events.

The acceptance of PAMELA is about 50 times smaller than AMS-02, however it has a neutron detector underneath the last scintillator layer, to improve the identification of hadronic interactions [84]. The neutron detector is located below the S4 scintillator and consists of 36 proportional counters, filled with ^3He and surrounded by a polyethylene moderator enveloped in a thin cadmium layer to prevent thermal neutrons entering the detector from the sides and from below. The neutron detector is active for 200 microseconds after each trigger, which is the time needed to thermalize neutrons produced by interactions of 20–180 GeV protons in the calorimeter [85]. As such, it seems that PAMELA is not able to perform a direct measurement of cosmic neutrons using the technique explained here.

Scintillators work well at the MeV scale or below, at which full absorption is possible. Arrays of scintillators similar to the CsI(Tl) crystals flown on *Salut-7* and *Kosmos-1686* orbital complex [86] might work also up to several GeV but this would require large volume and fine segmentation, which is not easy to obtain with this material.

Liquid scintillators are also good for discriminating neutron events from gamma-rays. For example, the omnidirectional neutron measurement by COMPTEL was performed using one D1 module, a cylinder with 13.8 cm radius and depth of 8 cm filled by liquid scintillator NE213A [43]. In addition to NE213 [87], other liquid scintillators are good, like the BC501A scintillator studied by the ICARUS collaboration [88], EJ301 (similar to BC501A), and the EJ309 scintillator, more suitable for environmentally difficult situations [89]. However, directionality is only achievable by developing a large time projection chamber filled by liquid scintillator, which is perhaps too challenging (though very interesting) for a space experiment.

A neutron detector design which exploits double n-p elastic collisions is SONTRAC [90], consisting of a set of orthogonal scintillating fibres (made by organic plastic scintillator) on top of a BGO calorimeter. However, its design is optimized to measure 20-250 MeV neutrons from solar flares. Thus, a much larger detector would be needed to reach the interesting energy regions for indirect WIMP detection. Imaida *et al.* [91] also developed a neutron detector made by scintillating fibres and a multi-anode photomultiplier, which was operated in space [22, 23]. Like SONTRAC, it covers the energy range interesting for solar flares. Moser *et al.* [92] also developed a stack of plastic scintillating fibres, in order to detect solar flare neutrons with n-p elastic scattering. They consider single-, double- and triple-scatter events up to about 100 MeV, but did not compute the full initial neutron momentum for any incoming direction, as we have done above. In the energy range useful for solar flares, arrays of plastic scintillator bars also work as fast neutron detectors [93]. At the price of a reduced granularity, they can cover wide surfaces. By stacking several layers, one may obtain a large-acceptance neutron detector with limited directionality.

Another interesting concept is HERO [94], although it is designed to detect thermalized neutrons about 100 μs after the trigger signal, similar to PAMELA, with the purpose of separating hadronic from electromagnetic showers. Still, its capability of reconstructing the cascade parameters gives it directional capability. What is missing is a trigger for neutral hadrons and an initial section of light active materials optimized for elastic scattering. Alexandrov *et al.* [95] proposed a ionization-neutron calorimeter, the INCA experiment, also designed to thermalize and detect neutrons. The primary purpose of INCA is the investigation of high-energy CR electrons and primary nuclei up to the knee region, hence it is a huge space project, with geometry close to 4π , $30\text{ m}^2\text{ sr}$ acceptance, and 10–12 t mass. However it is not optimized for the measurement of the cosmic neutron flux.

None of the detectors built or proposed so far is optimized for the measurement of the cosmic neutron flux over a broad energy range. As we have seen, at low energies elastic scattering is the main process, whereas at high energies inelastic collisions dominate. Hence one could design the instrument such that the face directed toward the source is optimized for elastic scattering, with a light active material, followed by a hadronic calorimeter made of a heavy material, for the reconstruction of hadronic showers.

The detector should have modular design, with multiple “towers” that can be tiled together. Alternatively, independent units may be installed, possibly on different satellites (in this case each unit will be sensitive to less energetic neutrons, compared to one big detector). A modular design simplifies the development, enhances the redundancy and fault tolerance, leaves some margin in case the overall mass or financial budget is downsized (in which case one might decide to build less units), and

allows for a gradual commissioning phase, in case independent units may be deployed in sequence.

The detector needs to be surrounded by an anticoincidence shield, in order to veto charged particles entering the active area from all directions. The anticoincidence system can be built with plastic scintillators, that provide a fast response with a high light yield and can be produced in a variety of shapes. Each tower must provide different response for neutrons and gamma-rays, in order to distinguish between them by means of pulse shape discrimination techniques.

Symmetric towers might also be developed, with sections optimized for elastic scattering on opposite sides. In this case, the detector can be pointed toward the Sun and simultaneously look at the opposite direction. Differential measurements have the potential for showing a modulation, for example when Jupiter or Mars are on the same side as the Sun or on the opposite side. Hence are more robust against systematics. For example, Jovian and Martian neutrons produced by CR interactions within their atmospheres, or neutrons coming from the Moon and produced by CR collision with the lunar soil, may be important sources of background. In principle, the reconstruction of the incoming neutron direction is sufficient to suppress this background. However, there might be some ambiguity or the experimental resolution may be not sufficient in all cases, and a differential measurements helps in keeping several sources of systematics under control.

The external segments of each tower shall provide the 3D position of the elastic scattering and allow for the reconstruction of the track left by the ejected proton. Organic plastic scintillators are available in the form of fibres with round or square cross-section, and are best suited for the first layers. Alternating layers with orthogonal fibres allow for the reconstruction of the location of the first collision (point A in figure 3) within about one fibre diameter (0.25 to 0.5 mm), and organic scintillators have a high fraction of hydrogen atoms, which are the best targets. The presence of carbon nuclei as additional targets for the n-C elastic scattering shall be taken into account, but the negligible amount of heavier elements makes these scintillators simpler to use than inorganic scintillators.

Liquid scintillators also provide a very good medium for elastic scattering, but reconstructing the proton track requires a time projection chamber, which is more complex (though a very attractive option) than a bundle of scintillating fibres. In addition, the layered structure of the latter makes it easy to implement the anticoincidence system, by configuring the trigger system in order to veto events with signals detected by the outermost fibres.

The organic scintillator fibres shall be followed by a segmented calorimeter, which is able to provide information on the shower shape in case of inelastic collision, and the position of the second neutron scattering (point B in figure 3) which has undergone an elastic collision in the external segment. A heavy material with relatively

short interaction length is the best choice, for example bismuth germanium oxide $\text{Bi}_4\text{Ge}_3\text{O}_{12}$ (or simply BGO). The total thickness along the line of sight of the instrument should be enough to guarantee the development of a hadronic shower, whose containment as a function of the neutron energy will determine the energy and direction resolution of the instrument.

Most hadronic detectors are sampling calorimeters, in which layers of heavy passive material (like tungsten or lead) are added to increase the interaction probability. The charged secondaries ionizing the active material are then detected, leaving measurable signals. In this case, the active material can be made of plastic scintillating fibres, which run most often along different directions, to provide a good position resolution. This alternative design is also worth consideration for two reasons. First, it has the advantage of using the same type of scintillator, hence also photon detector and associated electronics, for both light and heavy sections of each unit. Second, the layered structure provides information about the longitudinal direction, while heavy crystals would be coupled with photon detectors on one side only, making it almost impossible to obtain a 3-dimensional reconstruction.

After having discussed the guidelines for the design of a suitable detector, we conclude the section with the description of a compact demonstrator. We consider one unit consisting of a finely segmented calorimeter made of organic scintillating fibres, followed by one array of BGO crystals. The unit shall be equipped with an anticoincidence shield as shown in figure 4. The minimal size for covering at least the energy range of solar flare neutrons, while keeping volume and mass as low as possible, is close to a cubic $(20\text{ cm})^3$ fibre scintillator (8.5 kg) coupled with a box $(20 \times 20 \times 5)\text{ cm}^3$ containing BGO crystals (14.3 kg). By including anticoincidence scintillators, supporting mechanics, photon detector and related electronics, this payload would have mass in the range 30–40 kg, well within the capability of a small space mission. Pairing back-to-back two units and reaching a mass close to 70 kg, one would then obtain a bidirectional instrument, which is able to perform differential measurements, still within the range of a small space mission.

The nuclear collision length of BGO is 13.49 cm and the nuclear interaction length is 22.31 cm. One problem with this material is the short attenuation length (1.1 cm), which limits the maximum size of each crystal to few centimeters. For this reason, we consider here 5 cm thick crystals, which may have 2 cm width along two directions. This ensures a moderate granularity, 31% collision probability and 20% interaction probability, while achieving energy resolution of 16% at 511 keV and about 4000 photons from a minimum ionizing particle (depositing 8.92 MeV/cm) [2]. The radiation length is only 1.118 cm in BGO, hence the detection efficiency for gamma-rays is very high. This means that the same detector will also provide cosmic gamma-ray measurements of good quality, a valuable scientific bonus. In comparison, a segmented hadronic calorimeter would have worse

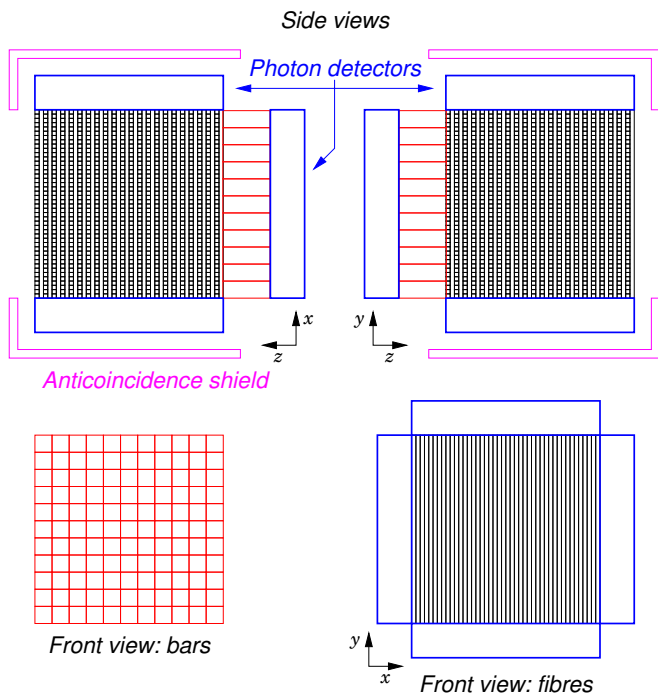


FIG. 4. Detector design principle. Scintillation fibre calorimeter (black) in front of crystal scintillator bars (red). Anticoincidence shield (magenta) surrounding the active detectors. Photon detectors (blue) are not shown for the anticoincidence scintillators.

performance in gamma-ray mode. This is the main reason why here the inorganic crystal calorimeter is considered for the demonstrator mission.

Organic scintillating fibres are available in several shapes and material. To make one example, 0.25 mm diameter fibres of BCF-10 by St. Gobain (essentially made of polystyrene) would provide an excellent spatial resolution and a high detection efficiency for charged particles. The external fibres may be configured in anticoincidence, vetoing all events in which a charged particle enters from the front face and complementing the work of the anticoincidence shield, which flags events with tracks entering the detector from the side. Neutrons have a collision probability of 31% in 20 cm polystyrene (the same as 5 cm BGO) and an interaction probability of 23%. Considering only neutrons that undergo one elastic scattering in the fibres and are detected by BGO thanks to another recoil or to a hadronic interaction (51% probability in total), this detector should have an efficiency of order 10%, to be estimated more accurately with Monte Carlo simulations.

The concept described above is very similar to SONTRAC, as it offers several layers of scintillating fibres alternating along orthogonal directions followed by BGO crystals. Hence the measured performance of the SONTRAC prototype [96] should provide a quite good reference for the demonstrator detector illustrated above, despite from the minor differences in geometry. The biggest

differences from SONTRAC are the bidirectional design, with scintillating fibres on two opposite faces to perform differential measurements, and the thicker BGO section, which increases the sampled energy range. In addition, this demonstrator may be considered one module of a bigger detector, whose main goal is not the study of solar flares but the search for DM induced neutrons with a high sensitivity. The actual instrument configuration (like dimensions, precise layout, photodetectors, etc.) shall be studied by means of Monte Carlo simulations, together with alternative designs (for example a sampling calorimeter with W layers alternating with scintillating fibres), in order to optimize the performance.

VI. SUMMARY

Cosmic neutrons can only reach the Earth if their energy is high enough that the relativistic time expansion effect ensures that they do not decay during their travel with high probability. For example, neutrons from the Sun need to have 20 MeV or higher energy. Neutrons from the closest supernova remnants can reach us only at PeV energies or above, in the knee region of the CR spectrum. Neutrons from the Galaxy center should have ultra high energy, affecting the CR ankle region.

Between solar neutrons, which can be emitted during a solar flare and are well correlated in time with the X-ray emission, and the other expected sources of cosmic neutrons, located well outside the solar system, there is a wide energy range in which the diffuse cosmic neutron flux should be not very dissimilar from the cosmic antiproton flux, which amounts to about 10^{-4} of CR protons. This is smaller than the secondary neutrons produced by CR interactions in the Earth atmosphere, at least over the energy range at which they have been already measured. Hence a directional detector operating in orbit is required, in order to get rid of this background.

A detector pointing to the Sun and able to measure the neutron flux also from the opposite side is proposed. It is also suggested to adopt several layers of orthogonal fibres of organic scintillators at the entrance sides, in order to study the kinematics of elastic collisions below few GeV, enclosing a heavier core in which inelastic interactions can produce hadronic showers. The central section may consist of BGO crystals, or be designed as a sampling calorimeter. This way, the neutron energy spectrum can be obtained at low energies by exploiting the kinematics of elastic n-p scattering as explained in section V A, and at high energies by adopting a hadronic calorimeter.

Charge particles shall be vetoed by an anticoincidence system, made with plastic scintillators surrounding the neutron detector. Gamma rays will be distinguished by means of pulse shape discrimination and by the shower development in the calorimeter. Finally, a modular design is possible, in which identical towers are tiled together.

Sun pointing is preferred for two reasons. In addition

to the possibility of detecting solar neutrons, which is important in understanding the acceleration mechanisms during solar flares, WIMP annihilations should be enhanced by the gravitational field of the Sun. This should increase the flux of neutrons entering from the Sun side, with respect to those entering from the dark side. In addition, the symmetric design is also motivated by the fact that differential measurements are robust against several sources of systematic effects. For example, the flux of secondary Jovian and Martian neutrons will show time variations according to their position. Any source of antiproton-proton signals will also produce antineutron-neutron pairs. Hence looking for an excess of cosmic neutrons is a very effective and low-background search for dark matter particles.

ACKNOWLEDGEMENTS

I'm grateful to Karel Kudela for the comments on the first draft of this paper and for pointing me to his ex-

cellent review of solar flare neutrons [97]. He also kindly provided me with valuable references, which I had no access to. Next, I wish to thank Marco Cirelli, who has verified the correctness of the assumption of similar production rates for neutrons and antiprotons and introduced me to PPPC 4 DM ID [98]. I also want to express my gratitude to Doojin Kim, for the discussion on the implications of DM “transporting” mechanisms [82] on cosmic neutrons. Finally I really appreciated the suggestions of the anonymous reviewer, which helped me to significantly improve this paper.

-
- [1] M. S. Longair, *High Energy Astrophysics*, 2nd ed., Vol. 1, 2 (Cambridge University Press, 1992, 1994).
- [2] C. Patrignani et al. (Particle Data Group) (Particle Data Group), *Chin. Phys.* **C40**, 100001 (2016).
- [3] S. Shibata, *J. Geophys. Res.* **99**, 6651 (1994).
- [4] A. O. Benz, *Living Rev. Solar Phys.* **5**, 1 (2008).
- [5] D. J. Forrest and E. L. Chupp, *Solar Phys.* **6**, 339 (1969).
- [6] W. N. Hess and R. C. Kaifer, *Solar Phys.* **2**, 202 (1967).
- [7] S. J. Bame and J. R. Asbridge, *J. Geophys. Res.* **71**, 4605 (1966).
- [8] E. L. Chupp, D. J. Forrest, J. M. Ryan, J. Heslin, C. Reppin, K. Pinkau, G. Kanbach, E. Rieger, and G. H. Share, *Astrophys. J.* **263**, L95 (1982).
- [9] F. B. McDonald and M. A. I. van Hollebeke, *Astrophys. J.* **290**, L67 (1985).
- [10] E. L. Chupp, H. Debrunner, E. Flueckiger, D. J. Forrest, F. Golliez, G. Kanbach, W. T. Vestrand, J. Cooper, and G. Share, *Astrophys. J.* **318**, 913 (1987).
- [11] H. Debrunner, E. Flueckiger, E. L. Chupp, and D. J. Forrest, in *Proc. 18th ICRC*, Vol. 4 (1983) pp. 75–78.
- [12] Y. E. Efimov, G. E. Kocharov, and K. Kudela, in *Proc. 18th ICRC*, Vol. 10 (Bangalore, India, 1983) pp. 276–278.
- [13] K. Kudela, *Astrophys. J. Suppl. Ser.* **73**, 297 (1990).
- [14] R. Ramaty, R. J. Murphy, B. Kozlovsky, and R. E. Lingenfelter, *Astrophys. J.* **273**, L41 (1983).
- [15] P. Evenson, P. Meyer, and K. R. Pyle, *Astrophys. J.* **274**, 875 (1983).
- [16] R. J. Murphy, C. D. Dermer, and R. Ramaty, *Astrophys. J. Suppl. Ser.* **63**, 721 (1987).
- [17] M. A. Shea, D. F. Smart, and K. R. Pyle, *Geophys. Res. Lett.* **18**, 1655 (1991).
- [18] H. Debrunner, J. A. Lockwood, C. Barat, R. Butikofer, J. P. Dezalay, E. Fluckiger, A. Kuznetsov, J. M. Ryan, R. Sunyaev, O. V. Terekhov, G. Trotter, and N. Vilmer, *Astrophys. J.* **479**, 997 (1997).
- [19] Y. Muraki, K. Murakami, M. Miyazaki, K. Mitsui, S. Shibata, S. Sakakibara, T. Sakai, T. Takahashi, T. Yamada, and K. Yamaguchi, *Astrophys. J.* **400**, L75 (1992).
- [20] N. Agueda, S. Krucker, R. P. Lin, and L. Wang, *Astrophys. J.* **737**, 53 (2011).
- [21] S. N. Kuznetsov, V. G. Kurt, B. Y. Yushkov, K. Kudela, and V. I. Galkin, *Solar Physics* **268**, 175 (2010).
- [22] Y. Muraki, D. Lopez, K. Koga, F. Kakimoto, T. Goka, L. X. González, S. Masuda, Y. Matsubara, H. Matsumoto, P. Miranda, O. Okudaira, T. Obara, J. Salinas, T. Sako, S. Shibata, R. Ticona, Y. Tsunesada, J. F. Valdés-Galicia, K. Watanabe, and T. Yamamoto, *Solar Phys.* **291**, 1241 (2016).
- [23] K. Koga, T. Goka, H. Matsumoto, T. Obara, Y. Muraki, and T. Yamamoto, *Astrophys. Space Sci. Trans.* **7**, 411 (2011).
- [24] X. X. Yu, H. Lu, G. T. Chen, X. Q. Li, J. K. Shi, and C. M. Tan, *New Astronomy* **39**, 25 (2015).
- [25] N. Hayashida, *Astropart. Phys.* **10**, 303 (1999).
- [26] A. Aab et al., *Astrophys. J.* **802**, 111 (2015).
- [27] R. W. Clay, *Publ. Astronom. Soc. Australia* **17**, 212 (2000).
- [28] R. L. Brown, *Astrophys. J.* **262**, 110 (1982).
- [29] A. Haungs, *Physics Procedia* **61**, 425 (2015), 13th International Conference on Topics in Astroparticle and Underground Physics.
- [30] J. Albert, E. Aliu, H. Anderhub, P. Antoranz, A. Armada, C. Baixeras, J. A. Barrio, H. Bartko, D. Bastieri, J. K. Becker, W. Bednarek, K. Berger, C. Bigongiari, A. Biland, R. K. Bock, P. Bordas, V. Bosch-Ramon, T. Bretz, I. Britvitch, M. Camara, E. Carmona, A. Chilingarian, J. A. Coarasa, S. Commichau, J. L. Contreras, J. Cortina, M. T. Costado, V. Curtef, V. Danielyan, F. Dazzi, A. De Angelis, C. Delgado, R. de los Reyes, B. De Lotto, E. Domingo-Santamaría, D. Dorner, M. Doro, M. Errando, M. Fagiolini, D. Fer-

- enc, E. Fernández, R. Firpo, J. Flix, M. V. Fonseca, L. Font, M. Fuchs, N. Galante, R. J. García-López, M. Garczarczyk, M. Gaug, M. Giller, F. Goebel, D. Hakobyan, M. Hayashida, T. Hengstebeck, A. Herrero, D. Höhne, J. Hose, C. C. Hsu, P. Jacon, T. Jogler, R. Kosyra, D. Kranich, R. Kritzer, A. Laille, E. Lindfors, S. Lombardi, F. Longo, J. López, M. López, E. Lorenz, P. Majumdar, G. Maneva, K. Mannheim, O. Mansutti, M. Mariotti, M. Martínez, D. Mazin, C. Merck, M. Meucci, M. Meyer, J. M. Miranda, R. Mirzoyan, S. Mizobuchi, A. Moralejo, D. Nieto, K. Nilsson, J. Ninkovic, E. Oña-Wilhelmi, N. Otte, I. Oya, M. Panniello, R. Paoletti, J. M. Paredes, M. Pasanen, D. Pascoli, F. Pauss, R. Pegna, M. Persic, L. Peruzzo, A. Piccioli, E. Prandini, N. Puchades, A. Raymers, W. Rhode, M. Ribó, J. Rico, M. Rissi, A. Robert, S. Rügamer, A. Saggion, T. Saito, A. Sánchez, P. Sartori, V. Scanzotto, V. Scapin, R. Schmitt, T. Schweizer, M. Shayduk, K. Shinozaki, S. N. Shore, N. Sidro, A. Sillanpää, D. Sobczynska, A. Stamerra, L. S. Stark, L. Takalo, P. Temnikov, D. Tescaro, M. Teshima, D. F. Torres, N. Turini, H. Vankov, V. Vitale, R. M. Wagner, T. Wibig, W. Wittek, F. Zandanel, R. Zanin, and J. Zapatero, *Astrophys. J. Lett.* **665**, L51 (2007).
- [31] M. Sikora, M. C. Begelman, and B. Rudak, *Astrophys. J.* **341**, L33 (1989).
- [32] W. Tkaczyk, *Astrophys. J. Suppl. Ser.* **92**, 611 (1994).
- [33] M. Wenger, F. Ochsenbein, D. Egret, P. Dubois, F. Bonnarel, S. Borde, F. Genova, G. Jasniewicz, S. Laloë, S. Lesteven, and R. Monier, *A&A Suppl. Series* **143**, 9 (2000).
- [34] Data from [33] summarized in https://en.wikipedia.org/wiki/List_of_supernova_candidates.
- [35] O. Adriani, G. C. Barbarino, G. A. Bazilevskaia, R. Bellotti, M. Boezio, E. A. Bogomolov, L. Bonechi, M. Bongio, V. Bonvicini, S. Borisov, S. Bottai, A. Bruno, F. Cafagna, D. Campana, R. Carbone, P. Carlson, M. Casolino, G. Castellini, L. Consiglio, M. P. D. Pascale, C. D. Santis, N. D. Simone, V. D. Felice, A. M. Galper, W. Gillard, L. Grishantseva, P. Hofverberg, G. Jerse, A. V. Karelin, S. V. Koldashov, S. Y. Krutkov, A. N. Kvashnin, A. Leonov, V. Malvezzi, L. Marcelli, A. G. Mayorov, W. Menn, V. V. Mikhailov, E. Mocchiutti, A. Monaco, N. Mori, N. Nikonov, G. Osteria, P. Papini, M. Pearce, P. Picozza, C. Pizzolotto, M. Ricci, S. B. Ricciarini, L. Rossetto, M. Simon, R. Sparvoli, P. Spillantini, Y. I. Stozhkov, A. Vacchi, E. Vannuccini, G. Vasilyev, S. A. Voronov, J. Wu, Y. T. Yurkin, G. Zampa, N. Zampa, and V. G. Zverev, *Phys. Rev. Lett.* **105**, 121101 (2010).
- [36] M. Aguilar and et al., *Phys. Rev. Lett.* **117**, 091103 (2016).
- [37] J. Alcaraz, D. Alvisi, B. Alpat, G. Ambrosi, H. Anderhub, L. Ao, A. Arefiev, P. Azzarello, E. Babucci, L. Baldini, M. Basile, D. Barancourt, F. Barao, G. Barbier, G. Barreira, R. Battiston, R. Becker, U. Becker, L. Belagamba, P. Béné, J. Berdugo, P. Berges, B. Bertucci, A. Biland, S. Bizzaglia, S. Blasko, G. Boella, M. Boschini, M. Bourquin, G. Bruni, M. Buenerd, J. D. Burger, W. J. Burger, X. D. Cai, R. Cavalletti, C. Camps, P. Canarsa, M. Capell, D. Casadei, J. Casaus, G. Castellini, Y. H. Chang, H. F. Chen, H. S. Chen, Z. G. Chen, N. A. Chernoplekov, A. Chiarini, T. H. Chiueh, Y. L. Chuang, F. Cindolo, V. Commichau, A. Contin, A. Cotta-Ramusino, P. Crespo, M. Cristinziani, J. P. da Cunha, T. S. Dai, J. D. Deus, N. Dinu, L. Djambazov, I. D'Antone, Z. R. Dong, P. Emonet, J. Engelberg, F. J. Eppling, T. Eronen, G. Esposito, P. Extermann, J. Favier, C. C. Feng, E. Fiandrini, F. Finelli, P. H. Fisher, R. Flamini, G. Fluegge, N. Fouque, Y. Galaktionov, M. Gervasi, P. Giusti, D. Grandi, W. Q. Gu, K. Hangarter, A. Hasan, V. Hermel, H. Hofer, M. A. Huang, W. Hungerford, M. Ionica, R. Ionica, M. Jongmanns, K. Karlamaa, W. Karpinski, G. Kenney, J. Kenny, W. Kim, A. Klimentov, R. Kossakowski, V. Koutsenko, G. Laborie, T. Laitinen, G. Lamanna, G. Laurenti, A. Lebedev, S. C. Lee, G. Levi, P. Levchenko, C. L. Liu, H. T. Liu, I. Lopes, G. Lu, Y. S. Lu, K. Lübelmeyer, D. Luckey, W. Lustermann, C. Maña, A. Margotti, F. Massera, F. Mayet, R. R. McNeil, B. Meillon, M. Menichelli, F. Mezzanotte, R. Mezzenga, A. Mihul, G. Molinari, A. Mourao, A. Mujunen, F. Palmonari, G. Pancaldi, A. Papi, I. H. Park, M. Pauluzzi, F. Pauss, E. Perrin, A. Pesci, A. Pevsner, R. Pilastrini, M. Pimenta, V. Plyaskin, V. Pojidaev, H. Postema, V. Postolache, E. Prati, N. Produit, P. G. Rancoita, D. Rapin, F. Raupach, S. Recupero, D. Ren, Z. Ren, M. Ribordy, J. P. Richeux, E. Riihonen, J. Ritakari, U. Roeser, C. Roissin, R. Sagdeev, D. Santos, G. Sartorelli, A. Schultz von Dratzig, G. Schwering, E. S. Seo, V. Shoutko, E. Shoumilov, R. Siedling, D. Son, T. Song, M. Steuer, G. S. Sun, H. Suter, X. W. Tang, S. C. C. Ting, S. M. Ting, M. Tornikoski, G. Torromeo, J. Torsti, J. Trümper, J. Ulbricht, S. Urpo, I. Usoskin, E. Valtonen, J. Vandenhirtz, F. Velcea, E. Velikhov, B. Verlaet, I. Vetlitsky, F. Vezzu, J. P. Vialle, G. Viertel, D. Vité, H. Von Gunten, S. Waldmeier Wicki, W. Wallraff, B. C. Wang, J. Z. Wang, Y. H. Wang, K. Wiik, C. Williams, S. X. Wu, P. C. Xia, J. L. Yan, L. G. Yan, C. G. Yang, M. Yang, S. W. Ye, P. Yeh, Z. Z. Xu, H. Y. Zhang, Z. P. Zhang, D. X. Zhao, G. Y. Zhu, W. Z. Zhu, H. L. Zhuang, and A. Zichichi, *Phys. Lett. B* **472**, 215 (2000).
- [38] J. Alcaraz, B. Alpat, G. Ambrosi, H. Anderhub, L. Ao, A. Arefiev, P. Azzarello, E. Babucci, L. Baldini, M. Basile, D. Barancourt, F. Barao, G. Barbier, G. Barreira, R. Battiston, R. Becker, U. Becker, L. Belagamba, P. Béné, J. Berdugo, P. Berges, B. Bertucci, A. Biland, S. Bizzaglia, S. Blasko, G. Boella, M. Boschini, M. Bourquin, L. Brocco, G. Bruni, M. Buenerd, J. D. Burger, W. J. Burger, X. D. Cai, C. Camps, P. Canarsa, M. Capell, D. Casadei, J. Casaus, G. Castellini, C. Cecchi, Y. H. Chang, H. F. Chen, H. S. Chen, Y. L. Chuang, N. A. Chernoplekov, T. H. Chiueh, Y. L. Chuang, F. Cindolo, V. Commichau, A. Contin, P. Crespo, M. Cristinziani, J. P. da Cunha, T. S. Dai, J. D. Deus, N. Dinu, L. Djambazov, I. D'Antone, Z. R. Dong, P. Emonet, J. Engelberg, F. J. Eppling, T. Eronen, G. Esposito, P. Extermann, J. Favier, E. Fiandrini, P. H. Fisher, G. Fluegge, N. Fouque, Y. Galaktionov, M. Gervasi, P. Giusti, D. Grandi, O. Grimm, W. Q. Gu, K. Hangarter, A. Hasan, V. Hermel, H. Hofer, M. A. Huang, W. Hungerford, M. Ionica, R. Ionica, M. Jongmanns, K. Karlamaa, W. Karpinski, G. Kenney, J. Kenny, W. Kim, A. Klimentov, R. Kossakowski, V. Koutsenko, M. Kraeber, G. Laborie, T. Laitinen, G. Lamanna, G. Laurenti, A. Lebedev, S. C. Lee, G. Levi, P. Levchenko, C. L. Liu, H. T. Liu, I. Lopes, G. Lu, Y. S. Lu, K. Lübelmeyer, D. Luckey, W. Lustermann,

- C. Maña, A. Margotti, F. Mayet, R. R. McNeil, B. Meillon, M. Menichelli, A. Mihul, A. Mourao, A. Mujuenen, F. Palmonari, A. Papi, I. H. Park, M. Pauluzzi, F. Pauss, E. Perrin, A. Pesci, A. Pevsner, M. Pimenta, V. Plyaskin, V. Pojidaev, V. Postolache, N. Produit, P. G. Rancoita, D. Rapin, F. Raupach, D. Ren, Z. Ren, M. Ribordy, J. P. Richeux, E. Riihonen, J. Ritakari, U. Roeser, C. Roissin, R. Sagdeev, G. Sartorelli, A. Schultz von Dratzig, G. Schwering, G. Scolieri, E. S. Seo, V. Shoutko, E. Shoumilov, R. Siedling, D. Son, T. Song, M. Steuer, G. S. Sun, H. Suter, X. W. Tang, S. C. C. Ting, S. M. Ting, M. Tornikoski, J. Torsti, J. Trümper, J. Ulbricht, S. Urpo, I. Usoskin, E. Valtonen, J. Vandenhiert, F. Velcea, E. Velikhov, B. Verlaet, I. Vetlitsky, F. Vezzu, J. P. Vialle, G. Viertel, D. Vité, H. Von Gunten, S. Waldmeier Wicki, W. Wallraff, B. C. Wang, J. Z. Wang, Y. H. Wang, K. Wiik, C. Williams, S. X. Wu, P. C. Xia, J. L. Yan, L. G. Yan, C. G. Yang, M. Yang, S. W. Ye, P. Yeh, Z. Z. Xu, H. Y. Zhang, Z. P. Zhang, D. X. Zhao, G. Y. Zhu, W. Z. Zhu, H. L. Zhuang, A. Zichichi, and B. Zimmermann, *Phys. Lett. B* **484**, 10 (2000).
- [39] O. Adriani, G. C. Barbarino, G. A. Bazilevskaya, R. Bellotti, M. Boezio, E. A. Bogomolov, M. Bongi, V. Bonvicini, S. Bottai, A. Bruno, F. Cafagna, D. Campana, R. Carbone, P. Carlson, M. Casolino, G. Castellini, C. De Donato, C. De Santis, N. De Simone, V. Di Felice, V. Formato, A. M. Galper, A. V. Karelin, S. V. Koldashov, S. Koldobskiy, S. Y. Krutkov, A. N. Kvashnin, A. Leonov, V. Malakhov, L. Marcelli, M. Martucci, A. G. Mayorov, W. Menn, M. Mergé, V. V. Mikhailov, E. Mocchiutti, A. Monaco, N. Mori, R. Munini, G. Osteria, F. Palma, B. Panico, P. Papini, M. Pearce, P. Picozza, M. Ricci, S. B. Ricciarini, R. Sarkar, V. Scotti, M. Simon, R. Sparvoli, P. Spillantini, Y. I. Stozhkov, A. Vacchi, E. Vannuccini, G. I. Vasilyev, S. A. Voronov, Y. T. Yurkin, G. Zampa, N. Zampa, and V. G. Zverev, *Astrophys. J. Lett.* **799**, L4 (2015).
- [40] V. V. Mikhailov, O. Adriani, G. Barbarino, G. A. Bazilevskaya, R. Bellotti, M. Boezio, E. A. Bogomolov, M. Bongi, V. Bonvicini, S. Bottai, A. Bruno, F. S. Cafagna, D. Campana, R. Carbone, P. Carlson, M. Casolino, G. Castellini, L. Consiglio, C. D. Santis, N. D. Simone, V. D. Felice, A. M. Galper, A. V. Karelin, S. V. Koldashov, S. Koldobsky, S. Y. Krutkov, A. N. Kvashnin, A. A. Leonov, V. V. Malakhov, L. Marcelli, M. Martucci, A. G. Mayorov, W. Menn, M. Merge, E. Mocchiutti, A. Monaco, N. Mori, R. Munini, G. Osteria, P. Papini, F. Palma, B. Panico, M. Pearce, P. Picozza, M. Ricci, S. B. Ricciarini, R. Sarkar, V. Scotti, M. Simon, R. Sparvoli, P. Spillantini, Y. I. Stozhkov, A. Vacchi, E. Vannuccini, G. I. Vasiliev, S. A. Voronov, Y. T. Yurkin, G. Zampa, and N. Zampa, *Journal of Physics: Conference Series* **675**, 032003 (2016).
- [41] A. Bruno, O. Adriani, G. Barbarino, G. Bazilevskaya, R. Bellotti, M. Boezio, E. Bogomolov, M. Bongi, V. Bonvicini, S. Bottai, F. Cafagna, D. Campana, P. Carlson, M. Casolino, G. Castellini, E. Christian, C. D. Donato, G. de Nolfo, C. D. Santis, N. D. Simone, V. D. Felice, A. Galper, A. Karelin, S. Koldashov, S. Koldobskiy, S. Krutkov, A. Kvashnin, A. Leonov, V. Malakhov, L. Marcelli, M. Martucci, A. Mayorov, W. Menn, M. Merg, V. Mikhailov, E. Mocchiutti, A. Monaco, N. Mori, R. Munini, G. Osteria, F. Palma, B. Panico, P. Papini, M. Pearce, P. Picozza, M. Ricci, S. Ricciarini, J. Ryan, R. Sarkar, V. Scotti, M. Simon, R. Sparvoli, P. Spillantini, S. Stochaj, Y. Stozhkov, A. Vacchi, E. Vannuccini, G. Vasilyev, S. Voronov, Y. Yurkin, G. Zampa, and N. Zampa, *Adv. Space Res.* **???**, ??? (2016).
- [42] A. Bogomolov, A. Dmitriev, I. Myagkova, S. Ryumin, O. Smirnova, and I. Sobolevsky, *Adv. Space Res.* **21**, 1801 (1998).
- [43] D. J. Morris, H. Aarts, K. Bennett, J. A. Lockwood, M. L. McConnell, J. M. Ryan, V. Schnfelder, H. Steinle, and X. Peng, *J. Geophys. Res.* **100**, 12243 (1995).
- [44] W. N. Hess, H. W. Patterson, R. Wallace, and E. L. Chupp, *Phys. Rev.* **116**, 445 (1959).
- [45] C. Eyles, A. Linney, and G. Rochester, *Planet. Space Sci.* **20**, 1915 (1972).
- [46] A. M. Preszler, G. M. Simnett, and R. S. White, *J. Geophys. Res.* **79**, 17 (1974).
- [47] G. Kanbach, C. Reppin, and V. Schnfelder, *J. Geophys. Res.* **79**, 5159 (1974).
- [48] G. D. Badhwar, J. E. Keith, and T. F. Cleghorn, *Radiat. Meas.* **33**, 235 (2001).
- [49] H. Matsumoto, T. Goka, K. Koga, S. Iwai, T. Uehara, O. Sato, and S. Takagi, *Radiat. Meas.* **33**, 321 (2001).
- [50] H. Koshiishi, H. Matsumoto, A. Chishiki, T. Goka, and T. Omodaka, *Radiat. Meas.* **42**, 1510 (2007).
- [51] T. W. Armstrong, K. C. Chandler, and J. Barish, *J. Geophys. Res.* **78**, 2715 (1973).
- [52] D. Morris, H. Aarts, K. Bennett, J. Lockwood, M. McConnell, J. Ryan, V. Schnfelder, H. Steinle, and G. Weidenspointner, *Adv. Space Res.* **21**, 1789 (1998).
- [53] G. M. Frye, P. P. Dunphy, E. L. Chupp, and P. Evenson, *Solar Phys.* **118**, 321 (1988).
- [54] Y. Hochberg, E. Kuflik, T. Volansky, and J. G. Wacker, *Phys. Rev. Lett.* **113**, 171301 (2014).
- [55] Salucci, P., Nesti, F., Gentile, G., and Frigerio Martins, C., *A&A* **523**, A83 (2010).
- [56] A computation carried on in the hypothesis of an ideal gas at constant temperature in a central classical gravitational field gives a radial density function proportional to $\exp(A/r)/r^2$, where $A = GMM_{\odot}/(k_B T)$ is a constant length. The temperature of the cosmic background radiation is 2.7 K and the that of the cosmic neutrino background is 2 K. The DM temperature shall be lower. At $T = 1$ K one gets $A = 5.55$ pc, while at 0.1 K one gets 55.5 pc, to make an example. Hence one may get a huge amplification of the DM density close to a massive object. The problem is that, due to the exponential dependence, any small uncertainty on the local interstellar density maps into a huge uncertainty on the amplified DM density at 1 AU from the Sun. This means that it's almost impossible to estimate the DM at the Earth from the DM density obtained with measurements of galactic parameters.
- [57] F. Mayet, A. Green, J. Battat, J. Billard, N. Bozorgnia, G. Gelmini, P. Gondolo, B. Kavanagh, S. Lee, D. Loomba, J. Monroe, B. Morgan, C. OHare, A. Peter, N. Phan, and S. Vahsen, *Phys. Rep.* **627**, 1 (2016).
- [58] R. Bernabei, P. Belli, F. Cappella, R. Cerulli, C. J. Dai, A. d'Angelo, H. L. He, A. Incicchitti, H. H. Kuang, J. M. Ma, F. Montecchia, F. Nozzoli, D. Prospero, X. D. Sheng, and Z. P. Ye, *Eur. Phys. J. C* **56**, 333 (2008).
- [59] R. Bernabei, P. Belli, F. Cappella, R. Cerulli, C. J. Dai, A. d'Angelo, H. L. He, A. Incicchitti, H. H. Kuang, X. H. Ma, F. Montecchia, F. Nozzoli, D. Prospero, X. D. Sheng, R. G. Wang, and Z. P. Ye, *Eur. Phys. J. C* **67**, 39 (2010).

- [60] G. Angloher, M. Bauer, I. Bavykina, A. Bento, C. Bucci, C. Ciemniak, G. Deuter, F. von Feilitzsch, D. Hauff, P. Huff, C. Isaila, J. Jochum, M. Kiefer, M. Kimmerle, J.-C. Lanfranchi, F. Petricca, S. Pfister, W. Potzel, F. Pröbst, F. Reindl, S. Roth, K. Rottler, C. Sailer, K. Schäffner, J. Schmalzer, S. Scholl, W. Seidel, M. v. Sivers, L. Stodolsky, C. Strandhagen, R. Strauß, A. Tanzke, I. Usherov, S. Wawoczny, M. Willers, and A. Zöller, *Eur. Phys. J. C* **72**, 1971 (2012).
- [61] R. Agnese, Z. Ahmed, A. J. Anderson, S. Arrenberg, D. Balakishiyeva, R. Basu Thakur, D. A. Bauer, J. Billard, A. Borgland, D. Brandt, P. L. Brink, T. Bruch, R. Bunker, B. Cabrera, D. O. Caldwell, D. G. Cerdano, H. Chagani, J. Cooley, B. Cornell, C. H. Crewdson, P. Cushman, M. Daal, F. Dejongh, E. do Couto e Silva, T. Doughty, L. Esteban, S. Fallows, E. Figueroa-Feliciano, J. Filippini, J. Fox, M. Fritts, G. L. Godfrey, S. R. Golwala, J. Hall, R. H. Harris, S. A. Hertel, T. Hofer, D. Holmgren, L. Hsu, M. E. Huber, A. Jastram, O. Kamaev, B. Kara, M. H. Kelsey, A. Kennedy, P. Kim, M. Kiveni, K. Koch, M. Kos, S. W. Leman, B. Loer, E. Lopez Asamar, R. Mahapatra, V. Mandic, C. Martinez, K. A. McCarthy, N. Mirabolfathi, R. A. Moffatt, D. C. Moore, P. Nadeau, R. H. Nelson, K. Page, R. Partridge, M. Pepin, A. Phipps, K. Prasad, M. Pyle, H. Qiu, W. Rau, P. Redl, A. Reisetter, Y. Ricci, T. Saab, B. Sadoulet, J. Sander, K. Schneck, R. W. Schnee, S. Scorza, B. Serfass, B. Shank, D. Speller, K. M. Sundqvist, A. N. Villano, B. Welliver, D. H. Wright, S. Yellin, J. J. Yen, J. Yoo, B. A. Young, and J. Zhang (CDMS Collaboration), *Phys. Rev. Lett.* **111**, 251301 (2013).
- [62] C. E. Aalseth, P. S. Barbeau, J. Colaresi, J. I. Collar, J. Diaz Leon, J. E. Fast, N. Fields, T. W. Hossbach, M. E. Keillor, J. D. Kephart, A. Knecht, M. G. Marino, H. S. Miley, M. L. Miller, J. L. Orrell, D. C. Radford, J. F. Wilkerson, and K. M. Yocum, *Phys. Rev. Lett.* **107**, 141301 (2011).
- [63] A. Natarajan, J. B. Peterson, T. C. Voytek, K. Spekkens, B. Mason, J. Aguirre, and B. Willman, *Phys. Rev. D* **88**, 083535 (2013).
- [64] D. Hooper and L. Goodenough, *Phys. Lett. B* **697**, 412 (2011).
- [65] T. Daylan, D. P. Finkbeiner, D. Hooper, T. Linden, S. K. Portillo, N. L. Rodd, and T. R. Slatyer, *Physics of the Dark Universe* **12**, 1 (2016).
- [66] C. Weniger, *J. Cosmology Astropart. Phys.* **2012**, 007 (2012).
- [67] M. Ackermann, M. Ajello, A. Albert, B. Anderson, W. B. Atwood, L. Baldini, G. Barbiellini, D. Bastieri, R. Bellazzini, E. Bissaldi, R. D. Blandford, E. D. Bloom, R. Bonino, E. Bottacini, T. J. Brandt, J. Bregeon, P. Bruel, R. Buehler, S. Buson, G. A. Caliandro, R. A. Cameron, R. Caputo, M. Caragiulo, P. A. Caraveo, C. Cecchi, E. Charles, A. Chekhtman, J. Chiang, G. Chiaro, S. Ciprini, R. Claus, J. Cohen-Tanugi, J. Conrad, A. Cuoco, S. Cutini, F. D'Ammando, A. de Angelis, F. de Palma, R. Desiante, S. W. Digel, L. Di Venere, P. S. Drell, A. Drlica-Wagner, C. Favuzzi, S. J. Fegan, A. Franckowiak, Y. Fukazawa, S. Funk, P. Fusco, F. Gargano, D. Gasparrini, N. Giglietto, F. Giordano, M. Giroletti, G. Godfrey, G. A. Gomez-Vargas, I. A. Grenier, J. E. Grove, S. Guiriec, M. Gustafsson, J. W. Hewitt, A. B. Hill, D. Horan, G. Jóhannesson, R. P. Johnson, M. Kuss, S. Larsson, L. Latronico, J. Li, L. Li, F. Longo, F. Loparco, M. N. Lovellette, P. Lubrano, D. Malyshev, M. Mayer, M. N. Mazziotta, J. E. McEnery, P. F. Michelson, T. Mizuno, A. A. Moiseev, M. E. Monzani, A. Morselli, S. Murgia, E. Nuss, T. Ohsugi, M. Orienti, E. Orlando, J. F. Ormes, D. Paneque, M. Pesce-Rollins, F. Piron, G. Pivato, S. Rainò, R. Rando, M. Razzano, A. Reimer, T. Reposeur, S. Ritz, M. Sánchez-Conde, A. Schulz, C. Sgrò, E. J. Siskind, F. Spada, G. Spandre, P. Spinelli, H. Tajima, H. Takahashi, J. B. Thayer, L. Tibaldo, D. F. Torres, G. Tosti, E. Troja, G. Vianello, M. Werner, B. L. Winer, K. S. Wood, M. Wood, G. Zaharijas, and S. Zimmer, *Phys. Rev. D* **91**, 122002 (2015).
- [68] H. Abdalla, A. Abramowski, F. Aharonian, F. Ait Benkhali, A. G. Akhperjanian, T. Andersson, E. O. Angüner, M. Arrieta, P. Aubert, M. Backes, A. Balzer, M. Barnard, Y. Becherini, J. Becker Tjus, D. Berge, S. Bernhard, K. Bernlöhr, E. Birsin, R. Blackwell, M. Böttcher, C. Boisson, J. Bolmont, P. Bordas, J. Bregeon, F. Brun, P. Brun, M. Bryan, T. Bulik, M. Capasso, J. Carr, S. Casanova, N. Chakraborty, R. Chalme-Calvet, R. C. G. Chaves, A. Chen, J. Chevalier, M. Chrétiens, S. Colafrancesco, G. Cologne, B. Condon, J. Conrad, C. Couturier, Y. Cui, I. D. Davids, B. Degrange, C. Deil, J. Devin, P. deWilt, A. Djannati-Ataï, W. Domainko, A. Donath, L. O. Drury, G. Dubus, K. Dutton, J. Dyks, M. Dyrda, T. Edwards, K. Egberts, P. Eger, J.-P. Ernenwein, S. Eschbach, C. Farnier, S. Fegan, M. V. Fernandes, A. Fiasson, G. Fontaine, A. Förster, S. Funk, M. Fürbiinger, S. Gabici, M. Gajdus, Y. A. Gallant, T. Garrigoux, G. Giavitto, B. Giebels, J. F. Gluckstein, D. Gottschall, A. Goyal, M.-H. Grondin, M. Grudzińska, D. Hadasch, J. Hahn, J. Hawkes, G. Heinzlmann, G. Henri, G. Hermann, O. Hervet, A. Hillert, J. A. Hinton, W. Hofmann, C. Hoischen, M. Holler, D. Horns, A. Ivascenko, A. Jacholkowska, M. Jamrozny, M. Janiak, D. Jankowsky, F. Jankowsky, M. Jingo, T. Jogler, L. Jouvin, I. Jung-Richardt, M. A. Kastendieck, K. Katarzyński, U. Katz, D. Kerszberg, B. Khélifi, M. Kieffer, J. King, S. Klepser, D. Klochkov, W. Kluźniak, D. Kolitzus, N. Komin, K. Kosack, S. Krakau, M. Kraus, F. Krayzel, P. P. Krüger, H. Laffon, G. Lamanna, J. Lau, J.-P. Lees, J. Lefaucheur, V. Lefranc, A. Lemièrre, M. Lemoine-Goumard, J.-P. Lenain, E. Leser, R. Liu, T. Lohse, M. Lorentz, I. Lypova, V. Marandon, A. Marcowith, C. Mariaud, R. Marx, G. Maurin, N. Maxted, M. Mayer, P. J. Meintjes, M. Meyer, A. M. W. Mitchell, R. Moderski, M. Mohamed, K. Morå, E. Moulin, T. Murach, M. de Naurois, F. Niederwanger, J. Niemiec, L. Oakes, P. O'Brien, H. Odaka, S. Ohm, M. Ostrowski, S. Öttl, I. Oya, M. Padovani, M. Panter, R. D. Parsons, M. Paz Arribas, N. W. Pekeur, G. Pelletier, C. Perennes, P.-O. Petrucci, B. Peyaud, S. Pita, H. Poon, D. Prokhorov, H. Prokoph, G. Pühlhofer, M. Punch, A. Quirrenbach, S. Raab, A. Reimer, O. Reimer, M. Renaud, R. de los Reyes, F. Rieger, C. Romoli, S. Rosier-Lees, G. Rowell, B. Rudak, C. B. Rulten, V. Sahakian, D. Salek, D. A. Sanchez, A. Santangelo, M. Sasaki, R. Schlickeiser, F. Schüssler, A. Schulz, U. Schwanke, S. Schwemmer, M. Settimo, A. S. Seyffert, N. Shafi, I. Shilon, R. Simoni, H. Sol, F. Spanier, G. Spengler, F. Spies, L. Stawarz,

- R. Steenkamp, C. Stegmann, F. Stinzling, K. Stycz, I. Sushch, J.-P. Tavernet, T. Tavernier, A. M. Taylor, R. Terrier, L. Tibaldo, M. Tluczykont, C. Trichard, R. Tuffs, J. van der Walt, C. van Eldik, B. van Soelen, G. Vasileiadis, J. Veh, C. Venter, A. Viana, P. Vincent, J. Vink, F. Voisin, H. J. Völk, T. Vuillaume, Z. Wadiasingh, S. J. Wagner, P. Wagner, R. M. Wagner, R. White, A. Wierzcholska, P. Willmann, A. Wörnlein, D. Wouters, R. Yang, V. Zabalza, D. Zaborov, M. Zacharias, A. A. Zdziarski, A. Zech, F. Zefi, A. Ziegler, and N. Żywucka (H.E.S.S. Collaboration), *Phys. Rev. Lett.* **117**, 151302 (2016).
- [69] D. Hooper, D. P. Finkbeiner, and G. Dobler, *Phys. Rev. D* **76**, 083012 (2007).
- [70] G. Dobler, *Astrophys. J.* **750**, 17 (2012).
- [71] O. Adriani, G. C. Barbarino, G. A. Bazilevskaya, R. Bellotti, A. Bianco, M. Boezio, E. A. Bogomolov, M. Bongi, V. Bonvicini, S. Bottai, A. Bruno, F. Cafagna, D. Campana, R. Carbone, P. Carlson, M. Casolino, G. Castellini, C. De Donato, C. De Santis, N. De Simone, V. Di Felice, V. Formato, A. M. Galper, A. V. Karelin, S. V. Koldashov, S. A. Koldobskiy, S. Y. Krutkov, A. N. Kvashnin, A. Leonov, V. Malakhov, L. Marcelli, M. Martucci, A. G. Mayorov, W. Menn, M. Mergé, V. V. Mikhailov, E. Mocchiutti, A. Monaco, N. Mori, R. Munini, G. Osteria, F. Palma, P. Papini, M. Pearce, P. Picozza, C. Pizzolotto, M. Ricci, S. B. Ricciarini, L. Rossetto, R. Sarkar, V. Scotti, M. Simon, R. Sparvoli, P. Spillantini, S. J. Stochaj, J. C. Stockton, Y. I. Stozhkov, A. Vacchi, E. Vannuccini, G. I. Vasilyev, S. A. Voronov, Y. T. Yurkin, G. Zampa, N. Zampa, and V. G. Zverev, *Phys. Rev. Lett.* **111**, 081102 (2013).
- [72] L. Accardo, M. Aguilar, D. Aisa, B. Alpat, A. Alvino, G. Ambrosi, K. Andeen, L. Arruda, N. Attig, P. Azzarello, A. Bachlechner, F. Barao, A. Barrau, L. Barrin, A. Bartoloni, L. Basara, M. Battarbee, R. Battiston, J. Bazo, U. Becker, M. Behlmann, B. Beischer, J. Berdugo, B. Bertucci, G. Bigongiari, V. Bindi, S. Bizzaglia, M. Bizzarri, G. Boella, W. de Boer, K. Bollweg, V. Bonnivard, B. Borgia, S. Borsini, M. J. Boschini, M. Bourquin, J. Burger, F. Cadoux, X. D. Cai, M. Capell, S. Caroff, G. Carosi, J. Casaus, V. Cascioli, G. Castellini, I. Cernuda, D. Cerreta, F. Cervelli, M. J. Chae, Y. H. Chang, A. I. Chen, H. Chen, G. M. Cheng, H. S. Chen, L. Cheng, A. Chikanian, H. Y. Chou, E. Choumilov, V. Choutko, C. H. Chung, F. Cindolo, C. Clark, R. Clavero, G. Coignet, C. Consolandi, A. Contín, C. Corti, B. Coste, Z. Cui, M. Dai, C. Delgado, S. Della Torre, M. B. Demirköz, L. Derome, S. Di Falco, L. Di Masso, F. Dimiccoli, C. Díaz, P. von Doetinchem, W. J. Du, M. Duranti, D. D’Urso, A. Eline, F. J. Epling, T. Eronen, Y. Y. Fan, L. Farnesini, J. Feng, E. Fiandrini, A. Fiasson, E. Finch, P. Fisher, Y. Galaktionov, G. Gallucci, B. García, R. García-López, H. Gast, I. Gebauer, M. Gervasi, A. Ghelfi, W. Gillard, F. Giovacchini, P. Goglov, J. Gong, C. Goy, V. Grabski, D. Grandi, M. Graziani, C. Guandalini, I. Guerri, K. H. Guo, D. Haas, M. Habiby, S. Haino, K. C. Han, Z. H. He, M. Heil, R. Henning, J. Hoffman, T. H. Hsieh, Z. C. Huang, C. Huh, M. Incagli, M. Ionica, W. Y. Jang, H. Jinch, K. Kanishev, G. N. Kim, K. S. Kim, T. Kirn, R. Kossakowski, O. Kounina, A. Kounine, V. Koutsenko, M. S. Krafczyk, S. Kunz, G. La Vacca, E. Laudi, G. Laurenti, I. Lazzizzera, A. Lebedev, H. T. Lee, S. C. Lee, C. Leluc, G. Levi, H. L. Li, J. Q. Li, Q. Li, Q. Li, T. X. Li, W. Li, Y. Li, Z. H. Li, Z. Y. Li, S. Lim, C. H. Lin, P. Lipari, T. Lippert, D. Liu, H. Liu, M. Lolli, T. Lomtadze, M. J. Lu, Y. S. Lu, K. Luebelmeyer, F. Luo, J. Z. Luo, S. S. Lv, R. Majka, A. Malinin, C. Mañá, J. Marín, T. Martin, G. Martínez, N. Masi, F. Massera, D. Maurin, A. Menchaca-Rocha, Q. Meng, D. C. Mo, B. Monreal, L. Morescalchi, P. Mott, M. Müller, J. Q. Ni, N. Nikonov, F. Nozzoli, P. Nunes, A. Obermeier, A. Oliva, M. Orcinha, F. Palmonari, C. Palomares, M. Paniccia, A. Papi, M. Pauluzzi, E. Pedreschi, S. Pensotti, R. Pereira, R. Pilastrini, F. Pilo, A. Piluso, C. Pizzolotto, V. Plyaskin, M. Pohl, V. Poireau, E. Postaci, A. Putze, L. Quadrani, X. M. Qi, P. G. Rancoita, D. Rapin, J. S. Ricol, I. Rodríguez, S. Rosier-Lees, L. Rossi, A. Rozhkov, D. Rozza, G. Rybka, R. Sagdeev, J. Sandweiss, P. Saouter, C. Sbarra, S. Schael, S. M. Schmidt, D. Schuckardt, A. Schulz von Dratzig, G. Schwering, G. Scolieri, E. S. Seo, B. S. Shan, Y. H. Shan, J. Y. Shi, X. Y. Shi, Y. M. Shi, T. Siedenburger, D. Son, F. Spada, F. Spinella, W. Sun, W. H. Sun, M. Tacconi, C. P. Tang, X. W. Tang, Z. C. Tang, L. Tao, D. Tescaro, S. C. C. Ting, S. M. Ting, N. Tomassetti, J. Torsti, C. Türkoğlu, T. Urban, V. Vagelli, E. Valente, C. Vannini, E. Valtonen, S. Vaurynovich, M. Vecchi, M. Velasco, J. P. Vialle, V. Vitale, G. Volpini, L. Q. Wang, Q. L. Wang, R. S. Wang, X. Wang, Z. X. Wang, Z. L. Weng, K. Whitman, J. Wienkenhöver, H. Wu, K. Y. Wu, X. Xia, M. Xie, S. Xie, R. Q. Xiong, G. M. Xin, N. S. Xu, W. Xu, Q. Yan, J. Yang, M. Yang, Q. H. Ye, H. Yi, Y. J. Yu, Z. Q. Yu, S. Zeissler, J. H. Zhang, M. T. Zhang, X. B. Zhang, Z. Zhang, Z. M. Zheng, F. Zhou, H. L. Zhuang, V. Zhukov, A. Zichichi, N. Zimmermann, P. Zuccon, and C. Zurbach (AMS Collaboration), *Phys. Rev. Lett.* **113**, 121101 (2014).
- [73] O. Adriani, G. C. Barbarino, G. A. Bazilevskaya, R. Bellotti, M. Boezio, E. A. Bogomolov, M. Bongi, V. Bonvicini, S. Borisov, S. Bottai, A. Bruno, F. Cafagna, D. Campana, R. Carbone, P. Carlson, M. Casolino, G. Castellini, L. Consiglio, M. P. De Pascale, C. De Santis, N. De Simone, V. Di Felice, A. M. Galper, W. Gillard, L. Grishantseva, G. Jerse, A. V. Karelin, S. V. Koldashov, S. Y. Krutkov, A. N. Kvashnin, A. Leonov, V. Malakhov, V. Malvezzi, L. Marcelli, A. G. Mayorov, W. Menn, V. V. Mikhailov, E. Mocchiutti, A. Monaco, N. Mori, N. Nikonov, G. Osteria, F. Palma, P. Papini, M. Pearce, P. Picozza, C. Pizzolotto, M. Ricci, S. B. Ricciarini, L. Rossetto, R. Sarkar, M. Simon, R. Sparvoli, P. Spillantini, S. J. Stochaj, J. C. Stockton, Y. I. Stozhkov, A. Vacchi, E. Vannuccini, G. Vasilyev, S. A. Voronov, J. Wu, Y. T. Yurkin, G. Zampa, N. Zampa, and V. G. Zverev, *Phys. Rev. Lett.* **106**, 201101 (2011).
- [74] M. Aguilar, D. Aisa, A. Alvino, G. Ambrosi, K. Andeen, L. Arruda, N. Attig, P. Azzarello, A. Bachlechner, F. Barao, A. Barrau, L. Barrin, A. Bartoloni, L. Basara, M. Battarbee, R. Battiston, J. Bazo, U. Becker, M. Behlmann, B. Beischer, J. Berdugo, B. Bertucci, G. Bigongiari, V. Bindi, S. Bizzaglia, M. Bizzarri, G. Boella, W. de Boer, K. Bollweg, V. Bonnivard, B. Borgia, S. Borsini, M. J. Boschini, M. Bourquin, J. Burger, F. Cadoux, X. D. Cai, M. Capell, S. Caroff, J. Casaus, V. Cascioli, G. Castellini, I. Cernuda, F. Cervelli, M. J. Chae, Y. H. Chang, A. I. Chen,

- H. Chen, G. M. Cheng, H. S. Chen, L. Cheng, A. Chikanian, H. Y. Chou, E. Choumilov, V. Choutko, C. H. Chung, C. Clark, R. Claverio, G. Coignet, C. Consolandi, A. Contin, C. Corti, B. Coste, Z. Cui, M. Dai, C. Delgado, S. Della Torre, M. B. Demirköz, L. Derome, S. Di Falco, L. Di Masso, F. Dimiccoli, C. Díaz, P. von Doetinchem, W. J. Du, M. Duranti, D. D'Urso, A. Eline, F. J. Eppling, T. Eronen, Y. Y. Fan, L. Farnesini, J. Feng, E. Fiandrini, A. Fiasson, E. Finch, P. Fisher, Y. Galaktionov, G. Gallucci, B. García, R. García-López, H. Gast, I. Gebauer, M. Gervasi, A. Ghelfi, W. Gillard, F. Giovacchini, P. Goglov, J. Gong, C. Goy, V. Grabski, D. Grandi, M. Graziani, C. Guandalini, I. Guerri, K. H. Guo, M. Habiby, S. Haino, K. C. Han, Z. H. He, M. Heil, J. Hoffman, T. H. Hsieh, Z. C. Huang, C. Huh, M. Incagli, M. Ionica, W. Y. Jang, H. Jinchi, K. Kanishev, G. N. Kim, K. S. Kim, T. Kirn, R. Kosakowski, O. Kounina, A. Kounine, V. Koutsenko, M. S. Krafczyk, S. Kunz, G. La Vacca, E. Laudi, G. Laurenti, I. Lazzizzera, A. Lebedev, H. T. Lee, S. C. Lee, C. Leluc, H. L. Li, J. Q. Li, Q. Li, Q. Li, T. X. Li, W. Li, Y. Li, Z. H. Li, Z. Y. Li, S. Lim, C. H. Lin, P. Lipari, T. Lippert, D. Liu, H. Liu, T. Lomtadze, M. J. Lu, Y. S. Lu, K. Luebelmeyer, F. Luo, J. Z. Luo, S. S. Lv, R. Majka, A. Malinin, C. Mañá, J. Marín, T. Martin, G. Martínez, N. Masi, D. Maurin, A. Menchaca-Rocha, Q. Meng, D. C. Mo, L. Morescalchi, P. Mott, M. Müller, J. Q. Ni, N. Nikonov, F. Nozzoli, P. Nunes, A. Obermeier, A. Oliva, M. Orcinha, F. Palmonari, C. Palomares, M. Paniccia, A. Papi, E. Pedreschi, S. Pensotti, R. Pereira, F. Pilo, A. Piluso, C. Pizzolotto, V. Plyaskin, M. Pohl, V. Poireau, E. Postaci, A. Putze, L. Quadrani, X. M. Qi, P. G. Rancoita, D. Rapin, J. S. Ricol, I. Rodríguez, S. Rosier-Lees, A. Rozhkov, D. Rozza, R. Sagdeev, J. Sandweiss, P. Saouter, C. Sbarra, S. Schael, S. M. Schmidt, D. Schuckardt, A. S. von Dratzig, G. Schwering, G. Scolieri, E. S. Seo, B. S. Shan, Y. H. Shan, J. Y. Shi, X. Y. Shi, Y. M. Shi, T. Siedenburger, D. Son, F. Spada, F. Spinella, W. Sun, W. H. Sun, M. Tacconi, C. P. Tang, X. W. Tang, Z. C. Tang, L. Tao, D. Tesaro, S. C. C. Ting, S. M. Ting, N. Tomassetti, J. Torsti, C. Türkoğlu, T. Urban, V. Vagelli, E. Valente, C. Vannini, E. Valtonen, S. Vaurynovich, M. Vecchi, M. Velasco, J. P. Vialle, L. Q. Wang, Q. L. Wang, R. S. Wang, X. Wang, Z. X. Wang, Z. L. Weng, K. Whitman, J. Wienkenhöver, H. Wu, X. Xia, M. Xie, S. Xie, R. Q. Xiong, G. M. Xin, N. S. Xu, W. Xu, Q. Yan, J. Yang, M. Yang, Q. H. Ye, H. Yi, Y. J. Yu, Z. Q. Yu, S. Zeissler, J. H. Zhang, M. T. Zhang, X. B. Zhang, Z. Zhang, Z. M. Zheng, H. L. Zhuang, V. Zhukov, A. Zichichi, N. Zimmermann, P. Zuccon, and C. Zurbach (AMS Collaboration), *Phys. Rev. Lett.* **113**, 121102 (2014).
- [75] J. Chang, J. H. Adams, H. S. Ahn, G. L. Bashindzhagyan, M. Christl, O. Ganel, T. G. Guzik, J. Isbert, K. C. Kim, E. N. Kuznetsov, M. I. Panasyuk, A. D. Panov, W. K. H. Schmidt, E. S. Seo, N. V. Sokol'skaya, J. W. Watts, J. P. Wefel, J. Wu, and V. I. Zatssepin, *Nature* **456**, 362 (2008).
- [76] A. A. Abdo, M. Ackermann, M. Ajello, W. B. Atwood, M. Axelsson, L. Baldini, J. Ballet, G. Barbiellini, D. Bastieri, M. Battelino, B. M. Baughman, K. Bechtol, R. Bellazzini, B. Berenji, R. D. Blandford, E. D. Bloom, G. Bogaert, E. Bonamente, A. W. Borgland, J. Bregeon, A. Brez, M. Brigida, P. Bruel, T. H. Burnett, G. A. Caliandro, R. A. Cameron, P. A. Caraveo, P. Carlson, J. M. Casandjian, C. Cecchi, E. Charles, A. Chekhtman, C. C. Cheung, J. Chiang, S. Ciprini, R. Claus, J. Cohen-Tanugi, L. R. Cominsky, J. Conrad, S. Cutini, C. D. Dermer, A. de Angelis, F. de Palma, S. W. Digel, G. Di Bernardo, E. do Couto e Silva, P. S. Drell, R. Dubois, D. Dumora, Y. Edmonds, C. Farnier, C. Favuzzi, W. B. Focke, M. Frailis, Y. Fukazawa, S. Funk, P. Fusco, D. Gaggero, F. Gargano, D. Gasparrini, N. Gehrels, S. Germani, B. Giebels, N. Giglietto, F. Giordano, T. Glanzman, G. Godfrey, D. Grasso, I. A. Grenier, M.-H. Grondin, J. E. Grove, L. Guillemot, S. Guiriec, Y. Hanabata, A. K. Harding, R. C. Hartman, M. Hayashida, E. Hays, R. E. Hughes, G. Jóhannesson, A. S. Johnson, R. P. Johnson, W. N. Johnson, T. Kamae, H. Katagiri, J. Kataoka, N. Kawai, M. Kerr, J. Knödlseeder, D. Kocevski, F. Kuehn, M. Kuss, J. Lande, L. Latronico, M. Lemoine-Goumard, F. Lugo, F. Loparco, B. Lott, M. N. Lovellette, P. Lubrano, G. M. Madejski, A. Makeev, M. M. Massai, M. N. Mazziotta, W. McConville, J. E. McEnery, C. Meurer, P. F. Michelson, W. Mitthumsiri, T. Mizuno, A. A. Moiseev, C. Monte, M. E. Monzani, E. Moretti, A. Morselli, I. V. Moskalenko, S. Murgia, P. L. Nolan, J. P. Norris, E. Nuss, T. Ohsugi, N. Omodei, E. Orlando, J. F. Ormes, M. Ozaki, D. Paneque, J. H. Panetta, D. Parent, V. Pelassa, M. Pepe, M. Pesce-Rollins, F. Piron, M. Pohl, T. A. Porter, S. Profumo, S. Rainò, R. Rando, M. Razzano, A. Reimer, O. Reimer, T. Reposeur, S. Ritz, L. S. Rochester, A. Y. Rodriguez, R. W. Romani, M. Roth, F. Ryde, H. F.-W. Sadrozinski, D. Sanchez, A. Sander, P. M. Saz Parkinson, J. D. Scargle, T. L. Schalk, A. Sellholm, C. Sgrò, D. A. Smith, P. D. Smith, G. Spandre, P. Spinelli, J.-L. Starck, T. E. Stephens, M. S. Strickman, A. W. Strong, D. J. Suson, H. Tajima, H. Takahashi, T. Takahashi, T. Tanaka, J. B. Thayer, J. G. Thayer, D. J. Thompson, L. Tibaldo, O. Tibolla, D. F. Torres, G. Tosti, A. Tramacere, Y. Uchiyama, T. L. Usher, A. Van Etten, V. Vasileiou, N. Vilchez, V. Vitale, A. P. Waite, E. Wallace, P. Wang, B. L. Winer, K. S. Wood, T. Ylinen, and M. Ziegler (Fermi LAT Collaboration), *Phys. Rev. Lett.* **102**, 181101 (2009).
- [77] Aharonian, F., Akhperjanian, A. G., Anton, G., Barres de Almeida, U., Bazer-Bachi, A. R., Becherini, Y., Behera, B., Bernlhr, K., Bochow, A., Boisson, C., Bolmont, J., Borrel, V., Brucker, J., Brun, F., Brun, P., Bhlcr, R., Bulik, T., Bsching, I., Boutelier, T., Chadwick, P. M., Charbonnier, A., Chaves, R. C. G., Cheesebrough, A., Chounet, L.-M., Clapson, A. C., Coignet, G., Dalton, M., Daniel, M. K., Davids, I. D., Degrange, B., Deil, C., Dickinson, H. J., Djannati-Ata, A., Domainko, W., Drury, L. O'C., Dubois, F., Dubus, G., Dyks, J., Dyrda, M., Egberts, K., Emmanoulopoulos, D., Espigat, P., Farnier, C., Feinstein, F., Fiasson, A., Frster, A., Fontaine, G., Fling, M., Gabici, S., Gallant, Y. A., Grard, L., Gerbig, D., Giebels, B., Glicenstein, J. F., Glck, B., Goret, P., Gring, D., Hauser, D., Hauser, M., Heinz, S., Heinzelmann, G., Henri, G., Hermann, G., Hinton, J. A., Hoffmann, A., Hofmann, W., Holleran, M., Hoppe, S., Horns, D., Jacholkowska, A., de Jager, O. C., Jahn, C., Jung, I., Katarzyski, K., Katz, U., Kaufmann, S., Kendziorra, E., Kerschhaggl, M., Khangulyan, D., Khlifi, B., Keogh, D., Kluniak, W., Kneiske, T., Komin, Nu., Kosack, K., Kossakowski, R., Lamanna,

- G., Lenain, J.-P., Lohse, T., Marandon, V., Martin, J. M., Martineau-Huynh, O., Marcowith, A., Masbou, J., Maurin, D., McComb, T. J. L., Medina, M. C., Moderski, R., Moulin, E., Naumann-Godo, M., de Naurois, M., Nedbal, D., Nekrassov, D., Nicholas, B., Niemiec, J., Nolan, S. J., Ohm, S., Olive, J.-F., de Oa Wilhelmi, E., Orford, K. J., Ostrowski, M., Panter, M., Paz Arribas, M., Pedalletti, G., Pelletier, G., Petrucci, P.-O., Pita, S., Phlhofer, G., Punch, M., Quirrenbach, A., Raubenheimer, B. C., Raue, M., Rayner, S. M., Reimer, O., Renaud, M., Rieger, F., Ripken, J., Rob, L., Rosier-Lees, S., Rowell, G., Rudak, B., Rulten, C. B., Ruppel, J., Sahakian, V., Santangelo, A., Schlickeiser, R., Schck, F. M., Schröder, R., Schwanke, U., Schwarzburg, S., Schwemmer, S., Shalchi, A., Sikora, M., Skilton, J. L., Sol, H., Spangler, D., Stawarz, J., Steenkamp, R., Stegmann, C., Stinzing, F., Superina, G., Szostek, A., Tam, P. H., Tavernet, J.-P., Terrier, R., Tibolla, O., Tluczykont, M., van Eldik, C., Vasileiadis, G., Venter, C., Venter, L., Vialle, J. P., Vincent, P., Vivier, M., Vlk, H. J., Volpe, F., Wagner, S. J., Ward, M., Zdziarski, A. A., and Zech, A., *A&A* **508**, 561 (2009).
- [78] T. Aramaki, S. Boggs, S. Bufalino, L. Dal, P. von Doetinchem, F. Donato, N. Fornengo, H. Fuke, M. Grefe, C. Hailey, B. Hamilton, A. Ibarra, J. Mitchell, I. Mogret, R. Ong, R. Pereira, K. Perez, A. Putze, A. Raklev, P. Salati, M. Sasaki, G. Tarle, A. Urbano, A. Vittino, S. Wild, W. Xue, and K. Yoshimura, *Phys. Rep.* **618**, 1 (2016).
- [79] M.-Y. Cui, Q. Yuan, Y.-L. S. Tsai, and Y.-Z. Fan, *Phys. Rev. Lett.* **118**, 191101 (2017).
- [80] A. Cuoco, M. Krämer, and M. Korsmeier, *Phys. Rev. Lett.* **118**, 191102 (2017).
- [81] T. Kobayashi, J. Nishimura, Y. Komori, and K. Yoshida, *Adv. Space Res.* **27**, 653 (2001).
- [82] D. Kim, J.-C. Park, and S. Shin, *Dark Matter "Transporting" Mechanism Explaining Positron Excesses*, Tech. Rep. CERN-TH-2017-036 (CERN, 2017) [arXiv:1702.02944 \[hep-ph\]](https://arxiv.org/abs/1702.02944).
- [83] C. Pioch, V. Mares, E. Vashenyuk, Y. Balabin, and W. Rühm, *NIM A* **626**, 51 (2011).
- [84] O. Adriani, G. Barbarino, G. Bazilevskaya, R. Bellotti, M. Boezio, E. Bogomolov, M. Bongi, V. Bonvicini, S. Bottai, A. Bruno, F. Cafagna, D. Campana, R. Carbone, P. Carlson, M. Casolino, G. Castellini, M. D. Pascale, C. D. Santis, N. D. Simone, V. D. Felice, V. Formato, A. Galper, U. Giaccari, A. Karelin, M. Kheymits, S. Koldashov, S. Koldobskiy, S. Krut'kov, A. Kvashnin, A. Leonov, V. Malakhov, L. Marcelli, M. Martucci, A. Mayorov, W. Menn, V. Mikhailov, E. Mocchiutti, A. Monaco, N. Mori, R. Munini, N. Nikonov, G. Osteria, P. Papini, M. Pearce, P. Picozza, C. Pizzolotto, M. Ricci, S. Ricciarini, L. Rossetto, R. Sarkar, M. Simon, R. Sparvoli, P. Spillantini, Y. Stozhkov, A. Vacchi, E. Vannuccini, G. Vasilyev, S. Voronov, J. Wu, Y. Yurkin, G. Zampa, N. Zampa, and V. Zverev, *Phys. Rep.* **544**, 323 (2014).
- [85] Y. I. Stozhkov, A. Basili, R. Bencardino, M. Casolino, M. P. D. Pascale, G. Furano, A. Menicucci, M. Minori, A. Morselli, P. Picozza, R. Sparvoli, R. Wischnewski, A. Bakaldin, A. M. Galper, S. V. Koldashov, M. G. Korotkov, V. V. Mikhailov, S. A. Voronov, Y. T. Yurkin, O. Adriani, L. Bonechi, M. Bongi, P. Papini, S. B. Ricciarini, P. Spillantini, S. Straulino, F. Tacetti, E. Vannuccini, G. Castellini, M. Boezio, M. Bonvicini, E. Mocchiutti, P. Schiavon, A. Vacchi, G. Zampa, N. Zampa, P. Carlson, J. Lund, J. Lundquist, S. Orsi, M. Pearce, G. C. Barbarino, D. Campana, G. Osteria, G. Rossi, S. Russo, M. Boscherini, W. Menn, M. Simonh, L. Bongiorno, M. Ricci, M. Ambriola, R. Bellotti, F. Cafagna, M. Circella, C. D. Marzo, N. Giglietto, N. Mirizzi, M. Romita, P. Spinelli, E. Bogomolov, S. Krutkov, G. Vasiljev, G. A. Bazilevskaya, A. N. Kvashnin, V. I. Logachev, V. S. Makhmutov, O. S. Maksumov, Y. I. Stozhkov, J. W. Mitchell, R. E. Streitmatter, and S. J. Stochaj, *Int. J. Mod. Phys. A* **20**, 6745 (2005).
- [86] E. Bogolubov, A. Koshelev, V. Mikerov, and A. Sviridov, *NIM A* **652**, 99 (2011).
- [87] J. Lee and C. Lee, *Nucl. Instrum. Methods A* **402**, 147 (1998).
- [88] F. Arneodo, P. Benetti, A. Bettini, A. di Tigliole, E. Calligaris, C. Carpanese, F. Casagrande, D. Cavalli, F. Cavanna, P. Cennini, S. Centro, A. Cesana, C. Chen, Y. Chen, D. Cline, O. Consorte, I. Mitri, R. Dolfini, A. Ferrari, A. Berzolari, K. He, X. Huang, Z. Li, F. Lu, J. Ma, G. Mannocchi, C. Matthey, F. Mauri, L. Mazzone, C. Montanari, R. Nardò, S. Otwinowski, S. Parlati, D. Pascoli, A. Pepato, L. Periale, G. Mortari, A. Piazzoli, P. Picchi, F. Pietropaolo, A. Rappoldi, G. Raselli, S. Resconi, J. Revol, M. Rossella, C. Rossi, C. Rubbia, P. Sala, D. Scannicchio, F. Sergiampietri, S. Suzuki, M. Terrani, P. Torre, S. Ventura, M. Verdecchia, C. Vignoli, G. Xu, Z. Xu, H. Wang, J. Woo, C. Zhang, Q. Zhang, and S. Zheng, *Nucl. Instrum. Methods A* **418**, 285 (1998).
- [89] J. Iwanowska, L. Swiderski, T. Krakowski, T. Kozlowski, M. Moszynski, and G. Pausch, in *2012 IEEE Nuclear Science Symposium and Medical Imaging Conference Record (NSS/MIC)* (Institute of Electrical and Electronics Engineers (IEEE), 2012).
- [90] C. Wunderer, D. Holslin, J. Macri, M. McConnell, and J. Ryan, in *Conference on the High Energy Radiation Background in Space. Workshop Record* (Institute of Electrical and Electronics Engineers (IEEE), 1997).
- [91] I. Imaida, Y. Muraki, Y. Matsubara, K. Masuda, H. Tsuchiya, T. Hoshida, T. Sako, T. Koi, P. Ramana-murthy, T. Goka, H. Matsumoto, T. Omoto, A. Takase, K. Taguchi, I. Tanaka, M. Nakazawa, M. Fujii, T. Kohno, and H. Ikeda, *Nucl. Instrum. Methods A* **421**, 99 (1999).
- [92] M. Moser, E. Flückiger, J. Ryan, J. Macri, and M. McConnell, *Adv. Space Res.* **36**, 1399 (2005).
- [93] L. Karsch, A. Bhm, K.-T. Brinkmann, L. Demirrs, and M. Pfluff, *Nucl. Instrum. Methods A* **460**, 362 (2001).
- [94] E. Atkin, L. Burylov, A. Chubenko, N. Kuznetsov, M. Merkin, R. Mukhamedshin, A. Pavlov, D. Podorozhny, A. Romanov, L. Sveshnikova, L. Tkachev, A. Turundaevsky, and A. Voronin, *Nucl. Phys. B (Proc. Suppl.)* **196**, 450 (2009).
- [95] K. Alexandrov, M. Ambrosio, V. Ammosov, V. Antonova, C. Aramo, V. Bonvicini, V. Chechin, A. Chubenko, V. Drobzhnev, A. Erlykin, M. Fujii, Y. Hatano, S. Kryukov, E. Ladygin, B. Lomonosov, G. Merzon, R. Mukhamedshin, V. Murashov, V. Pavlyuchenko, M. Panasyuk, T. Roganova, A. Roussetski, V. Ryabov, O. Ryazhskaya, T. Saito, H. Sasaki, A. Shchepetov, N. Sobolevskii, N. Starkov, L. Sveshnikova, I. Trostin, V. Tsarev, A. Vacchi, A. Wolfendale, T. Yanagita, G. Zatsepin, G. Zhdanov, and A. Zhukov,

- [Nucl. Instrum. Methods A **459**, 135 \(2001\).](#)
- [96] J. M. Ryan, J. Baltgalvis, D. T. Holslin, J. R. Macri, M. L. McConnell, A. R. Polichar, and C. B. Wunderer, in *EUV, X-Ray, and Gamma-Ray Instrumentation for Astronomy VIII*, Vol. Vol. 3114, edited by O. H. W. Siegmund and M. A. Gummin (SPIE, 1997) pp. 514–525.
- [97] K. Kudela, *Acta Physica Slovaca* **59**, 537 (2009).
- [98] M. Cirelli, G. Corcella, A. Hektor, G. Htsi, M. Kadastik, P. Panci, M. Raidal, F. Sala, and A. Strumia, *Journal of Cosmology and Astroparticle Physics* **2011**, 051 (2011).